

E-Cigarette (E-Cig) Liquid Composition and Operational Voltage Define the *In Vitro* Toxicity of Δ^8 Tetrahydrocannabinol/Vitamin E Acetate (Δ^8 THC/VEA) E-Cig Aerosols

Antonella Marrocco ,* Dilpreet Singh,* David C. Christiani,* and Philip Demokritou*,†,1

*Department of Environmental Health, Center for Nanotechnology and Nanotoxicology, Harvard T.H. Chan School of Public Health, Harvard University, Boston, Massachusetts 02115, USA; and †Department of Environmental and Population Health Bio-Sciences, Environmental Occupational Health Sciences Institute, School of Public Health, Rutgers University, Piscataway, New Jersey 08854, USA

¹To whom correspondence should be addressed at Department of Environmental Health, Center for Nanotechnology and Nanotoxicology, Harvard T.H. Chan School of Public Health, Harvard University, 665 Huntington Avenue, Building 1, Room 1310, Boston, MA 02115, USA. E-mail: pdemokri@hsph.harvard.edu.

ABSTRACT

The 2019 United States outbreak of E-cigarette (e-cig), or Vaping, Associated Acute Lung Injury (EVALI) has been linked to presence of vitamin E acetate (VEA) in Δ^8 tetrahydrocannabinol (Δ^8 THC)-containing e-liquids, as supported by VEA detection in patient biological samples. However, the pathogenesis of EVALI and the complex physicochemical properties of e-cig emissions remain unclear, raising concerns on health risks of vaping. This study investigates the effect of Δ^8 THC/VEA e-liquids and e-cig operational voltage on *in vitro* toxicity of e-cig aerosols. A novel E-cigExposure Generation System platform was used to generate and characterize e-cig aerosols from a panel of Δ^8 THC/VEA or nicotine-based e-liquids at 3.7 or 5 V. Human lung Calu-3 cells and THP-1 monocytes were exposed to cell culture media conditioned with collected e-cig aerosol condensate at doses of 85 and 257 puffs/m² lung surface for 24 h, whereafter specific toxicological endpoints were assessed (including cytotoxicity, metabolic activity, reactive oxygen species generation, apoptosis, and inflammatory cytokines). Higher concentrations of gaseous volatile organic compounds were emitted from Δ^8 THC/VEA compared with nicotine-based e-liquids, especially at 5 V. Emitted PM_{2.5} concentrations in aerosol were higher for Δ^8 THC/VEA at 5 V and averagely for nicotine-based e-liquids at 3.7 V. Overall, aerosols from nicotine-based e-liquids showed higher bioactivity than Δ^8 THC/VEA aerosols in THP-1 cells, with no apparent differences in Calu-3 cells. Importantly, presence of VEA in Δ^8 THC and menthol flavoring in nicotine-based e-liquids increased cytotoxicity of aerosols across both cell lines, especially at 5 V. This study systematically investigates the physicochemical and toxicological properties of a model of Δ^8 THC/VEA and nicotine e-cigarette condensate exposure demonstrating that pyrolysis of these mixtures can generate hazardous toxicants whose synergistic actions potentially drive acute lung injury upon inhalation.

Key words: EVALI e-cigs vaping acute lung injury; e-cigs aerosols nanoparticles; e-cigs aerosols ultrafine particles; e-cigs aerosol lung toxicity; e-cigs aerosols respiratory effects.

The “E-cigarette (e-cig), or Vaping, Associated Acute Lung Injury” or EVALI outbreak started in the United States in July 2019 and lasted until February 18, 2020, when the Centers for Disease Control and Prevention (CDC) ended case reporting as the SARS-COV-2 pandemic arose in the United States. The outbreak led to 2807 hospitalizations, including 68 deaths. The EVALI outbreak raised public health concerns on the health risks associated with vaping, especially among the younger population (CDC, 2020). Due to the heterogeneity of clinical signs and symptoms that accompany the alveolar damage and hypoxemia, the diagnosis of EVALI is made by excluding any other possible cause of acute lung injury, such as infection or alternative diagnosis, in patients that used e-cigs in the 90 days before the onset of the symptoms, and presented with pulmonary infiltrates on chest radiograph or ground-glass opacities on chest computed tomography (CDC, 2019). The analysis performed on biological samples of EVALI patients, such as bronchoalveolar lavage (BAL) (Blount et al., 2019; Taylor et al., 2019), and e-cig products, including vaping devices, e-liquids, packaging, or other documentation (FDA, 2020), showed that the primary e-liquid constituents were Δ^9 tetrahydrocannabinol (Δ^9 THC) and vitamin E acetate (VEA) (Blount et al., 2020; Duffy et al., 2020; FDA, 2020; Muthumalage et al., 2020a; Taylor et al., 2019), whereas nicotine vaping alone was found only in a small percentage of cases (Blount et al., 2020; FDA, 2020; Taylor et al., 2019).

From the limited investigations on the e-cigs provided by EVALI patients, there was clearly a substantial difference between the marijuana medical products (MMP) and the EVALI cartridges. Although the conventional MMP contained Δ^9 THC 80%–90% + Terpenes 10%–20%, the EVALI cartridges contained <50% Δ^9 THC, due to increased Δ^8 THC, leading to an unusual ratio of Δ^9 THC/ Δ^8 THC isomers. Additional numerous other chemicals, including VEA in a concentration range of 16%–88% (most commonly 16%–58%) or medium-chain triglyceride (MCT, concentration range 3%–24%) (Duffy et al., 2020; FDA, 2020; Muthumalage et al., 2020a), pesticide residues, terpenes, manufacturing/pesticides/automotive chemicals (eg, *n*-butane, benzene, xylene, pentane, etc.), solvents (eg, ethanol, acetone, ethylbenzene, toluene, etc.), PCP-polycaprolactone/household chemicals (eg, methacrolein, acetaldehyde, etc.), other toxic compounds (eg, acrolein, penta-diene compounds, hexane compounds, methyl vinyl ketone, etc.), and elements included Si, Cu, Ni, and Pb (Muthumalage et al., 2020a), were unexpectedly present.

To date, efforts have focused on characterizing vaping emissions from nicotine-based e-liquids either physicochemically or toxicologically (Zhao et al., 2016, 2018a), whereas the literature regarding Δ^8 THC/VEA-based e-liquids is very scarce. Hence, the causative agent or mechanism underlying EVALI is still unknown. Indeed, the majority of studies focused only on the physicochemical characterization (Jiang et al., 2020; Lanzarotta et al., 2020; Meehan-Atrash et al., 2019; Mikheev et al., 2020) or biological *in vivo/in vitro* assessment (Bhat et al., 2020; Jiang et al., 2020; Matsumoto et al., 2020; Muthumalage et al., 2020b; Muthumalage and Rahman, 2019) of e-liquids or aerosols generated from a single e-liquid compound (ie, THC or VEA or other additives), which is not representative of e-liquids used by e-cig consumers.

The physical, chemical, and toxicological properties of e-cig emissions depend on many variables, consisting of e-liquid composition, device type (coil material, power supply, voltage, temperature), and puffing topography (CDC U.S. Department of Health and Human Services 2016; Zhao et al., 2016, 2018a,b). However, due to the lack of regulations on the manufacturing and commercialization of e-cigs, the e-liquids and devices are widely customizable, causing the generation of a variety of

chemical mixtures in the e-cig aerosols, in which the toxic components can potentially exert synergistic effects in the development of the EVALI syndrome.

The novel E-cig-Exposure Generation System (E-cig-EGS) platform was used to perform a systematic investigation of aerosols generated from combinations of Δ^8 THC/VEA/terpenes at various real-world concentrations, compared with nicotine-based e-liquids, linking the generation parameters to physicochemical properties of aerosols, using state-of-the-art analytical methods. Consequently, the biological and toxicological assessment of each sampled aerosol was performed using 2 physiologically relevant cell lines, Calu-3 epithelial cells, and THP-1 monocyte, which represent the first line of defense in the airways against particle and toxicants released in the e-cig aerosols, and thus are more involved in the pathogenesis of acute lung injury. Several important endpoints were analyzed for understanding mechanisms of toxicity (eg, cell viability, reactive oxygen species (ROS) generation, mitochondrial dysfunction, activation of caspase-3, and release of pro- and anti-inflammatory biomarkers).

Although the most psychoactive cannabis derivative is Δ^9 THC, due to federal restrictions on research-use of cannabis products, this study tested Δ^8 THC as a surrogate of Δ^9 THC. Although chemically the 2 are close, their toxicological profiles may differ. Moreover, the fact that Δ^8 THC escapes the FDA and other potential state regulations, by being manufactured from legal hemp-derived cannabidiol (CBD), increases its popularity and use especially in e-liquids, even though they have not been evaluated or approved by the FDA for safe use in any circumstance (NIDA, 2021, September 20).

This study is among the first to systematically investigate the physicochemical properties and cellular toxicity of Δ^8 THC/VEA and nicotine aerosols, with the goal of understanding and quantifying the risks of exposure to e-cig emissions, and more importantly, elucidating the mechanistic aspects driving the development of EVALI.

MATERIALS AND METHODS

E-cig Cartridges and E-liquids

The Δ^8 THC/VEA e-cigs were prepared using the following materials: CCell cartridge 510 thread (1 ml) (Hamilton Devices, Sacramento, California), Δ^8 THC, (+/–)- α -tocopherol acetate (VEA) (cat. no. T3376-100G, Sigma-Aldrich), lab-prepared mixture of terpenes (Terp) containing an equal concentration of myrcene (cat. no. W276212-100G-K, Sigma-Aldrich), caryophyllene (cat. no. 22075-5ML-F, Sigma-Aldrich), limonene (cat. no. 183164-100ML, Sigma-Aldrich), and pinene (cat. no. CRM40339, Sigma-Aldrich).

The nicotine-based e-cigs were prepared using the following materials: KangerTech refillable cartridges T3S series clear cartomizer 1.8 ohm (Rock Bottom Vapes, LLC, Longwood, Florida), nicotine (cat. no. 470301-868, VWR), propylene glycol (PG) high purity (cat. no. 97061-956, VWR), glycerol (vegetable glycerin, VG), lab reagent (cat. no. BDH1172-1LP, VWR), and menthol (cat. no. 470301-734, VWR).

The refillable cartridges were filled with 0.8 ml of e-liquid composed of a combination of Δ^8 THC/VEA/Terp (4 Δ^8 THC/VEA e-cigs) or nicotine/PV/VG/menthol (3 nicotine-based e-cigs) in varying proportions and were operated at e-cig operating voltage 3.7 or 5 V, as listed in Supplementary Table 1. All the Δ^8 THC/VEA and nicotine-based e-liquid constituents and cartridges were prepared and kindly provided by Jeff Rawson PhD, Postdoctoral

Fellow from the Whitesides Laboratory, Department of Chemistry and Chemical Biology, Harvard University.

E-cig Exposure Generation System

The recent E-cig-EGS platform developed by the authors was used to generate real-world e-cig aerosol exposures for real-time monitoring and detailed physicochemical and toxicological characterization, as shown in Figure 1 (Zhao et al., 2016). Briefly, a fully programmable single-port e-cig generator (ECAG; e_Aerosols LLC, Central Valley, New York) was connected to the desired e-cig cartridge to generate exposures under precisely controlled puffing patterns and operational voltage. The generated e-cig aerosol was mixed and diluted with HEPA-filtered and activated charcoal-filtered ambient air in a 7-l cylindrical environmental chamber. The residence time of the aerosol in the chamber was set to 60 s to mimic lung “washout time” during active vaping in e-cig users (Invernizzi et al., 2007). The temperature and relative humidity of the chamber was controlled at 24°C and 90% respectively. The E-cig-EGS was connected with real-time and time-integrated monitoring and sampling instrumentation for physicochemical and toxicological characterization (Demokritou et al., 2004; Pal et al., 2015).

The E-cig-EGS was connected to the prefilled cartridge as described previously. A modified puffing protocol was applied, with a puff volume of 55 ml, puff duration of 4 s, and an interval of 30 s between consecutive puffs, reflecting real-world e-cig consumer behaviors (Farsalinos et al., 2013a; Zhao et al., 2016; 2018a).

Real-Time Monitoring of E-Cig Emissions

After aerosol mixing in the environmental chamber, the released particulate matter (PM) number concentration in the e-cig aerosol and its number-size distribution were simultaneously monitored. A scanning mobility particle sizer spectrometer (NanoScan SMPS, Model 3910; TSI Inc., Shoreview, Minnesota) was used to measure nano-PNC as a function of mobility particle diameter (MPD) in the range of 10–420 nm. An aerodynamic particle sizer spectrometer (APS, Model 3321; TSI Inc.) was used to measure PNC as a function of APD in the range of 0.5–20 µm. For both SMPS and APS, the intersample duration was set to 60 s, the same as the aerosol residence time in the environmental chamber.

In addition, the gaseous byproducts in the e-cig aerosol (CO and CO₂) and the environmental conditions (temperature and relative humidity) in the chamber were monitored using Q-Trak Indoor Air Quality (IAQ) Monitor (Model 8551, TSI Inc.) every 1 min. The total volatile organic compound (tVOC) levels were also measured using a photoionization detector sensor (TG-502 probe, GrayWolf Sensing Solutions, Shelton, Connecticut), equipped with a sensitive ppb-level probe, with a sample collected every 10 s. Background measurements of each parameter were collected for at least 2 min before the beginning of each aerosol generation/sampling experiment to ensure a stable, clean background. Real-time monitoring of e-cig emissions was assessed for a total of 10 min after the start of the puffing protocol.

Sampling of e-cig emissions. After 10 min of real-time monitoring following the initiation of the puffing protocol, the e-cig aerosol from the environmental chamber was bubbled through a fritted-head impinger (porosity A [145–174 µm] tip; Ace Glass Inc., Vineland, New Jersey) containing 20 ml of cell culture medium, either Eagle’s minimum essential medium (EMEM, American Type Culture Collection, ATCC, Rockville, Maryland) or Roswell Park Memorial Institute (RPMI) 1640 Medium (Gibco

BRL, Rockville, Maryland) for subsequent *in vitro* toxicological characterization. The impinger sampling flow rate was set to 0.2 l/min and the sampling duration was 30 min. Immediately following sampling, the culture media were aliquoted in 15 ml falcon tubes and stored at 4°C until cell exposure.

In addition, the generated PM in the e-cig aerosol was size fractionated and sampled using the 30 l/min Harvard Compact Cascade Impactor (CCI) (Demokritou et al., 2004) and characterized for mass concentration as a function of size by gravimetric analysis. Three substrates (Teflon filter for PM_{0.1} and polyurethane foams [PUF] for PM_{0.1–2.5} and PM_{>2.5} size fractions) were used to sample PM in the CCI. Before and after sampling, the PUFs and Teflon filters were weighed using a Mettler Toledo XPE analytical microbalance (Mettler-Toledo LLC, Columbus, Ohio, USA). The weight difference was calculated and normalized to determine the average PM mass concentration (mg/m³) corresponding to each size fraction in the e-cig aerosol.

Cell Culture and Exposure

Human lung epithelial cell line Calu-3 and human peripheral blood monocytes THP-1 cells, (ATCC), were cultured in Eagle’s EMEM medium (ATCC) and Roswell Park Memorial Institute (RPMI) 1640 Medium (Gibco BRL), respectively, supplemented with 10% fetal bovine serum, 100 U/ml of penicillin G and 100 mg/ml streptomycin and grown at 37°C in 5% CO₂.

Cells (passage number between 2 and 8) were seeded in 96-well plates at a density of 0.5 × 10⁶ cells/ml in 100 µl growth medium for a single well and exposed for 24 h. Both cell lines were exposed to 2 doses of the conditioned cell culture media generated with 85 and 257 puffs/m² of e-cig aerosol for the basic cytotoxicity assays, whereas the higher dose was administered for the acute inflammatory biomarker assessment (see below on dose justification). Untreated cells were used as a negative control. Conventional cigarette smoke sampled in the appropriate cell culture medium was used as a comparator in all cellular toxicological experiments. The smoke generated from an entire cigarette was bubbled directly into the impinger containing 20 ml of EMEM or RPMI medium, connected to a pump with a flow rate of 0.2 l/min (Supplementary Figure 1). The schematic for cigarette smoke sampling methodology is shown in Supplementary Figure 1. All cellular exposures were done using 3 independent biological samples and 3 technical replicates.

Cellular dose justification. The exposures in this study were large bolus doses of conditioned media generated with 85 and 257 puffs/m² of e-cig aerosol for 24 h. These doses were selected to mimic 1 and 3 months of vaping and were calculated based on the approximate number of puffs reported by e-cig users: 13 puffs/vaping session (Farsalinos et al., 2013b) or 120–180 puffs/day (Etter and Bullen, 2011; Kosmider et al., 2018; Tackett et al., 2015). The average of 200 puffs/day was normalized on the total exposure area of lung epithelial cells in an adult, which is 70 m². The resulting 2.85 puffs/m²/day represents the number of puffs that reaches each square meter area of lung surface each day, in an adult that vapes 200 puffs/day. Then we calculated the number of puffs vaped over a period of 30 and 90 days (1 and 3 months), which resulted in 6000 and 18 000 puffs, respectively. Thus, the target cellular exposure concentrations corresponding to 1 month and 3 months of vaping were calculated to be 85 and 257 puffs/m², respectively (eg 2.85 puffs/m² × 30 days = 85.5 puffs/m² which is equal to 6000 puffs in 30 days/70 m² = 85.7 puffs/m²). Subsequently, the volume of stock solution to be administered in bolus for 24 h was determined based on the e-cig aerosol concentration (units of puffs/ml) in the stock solution

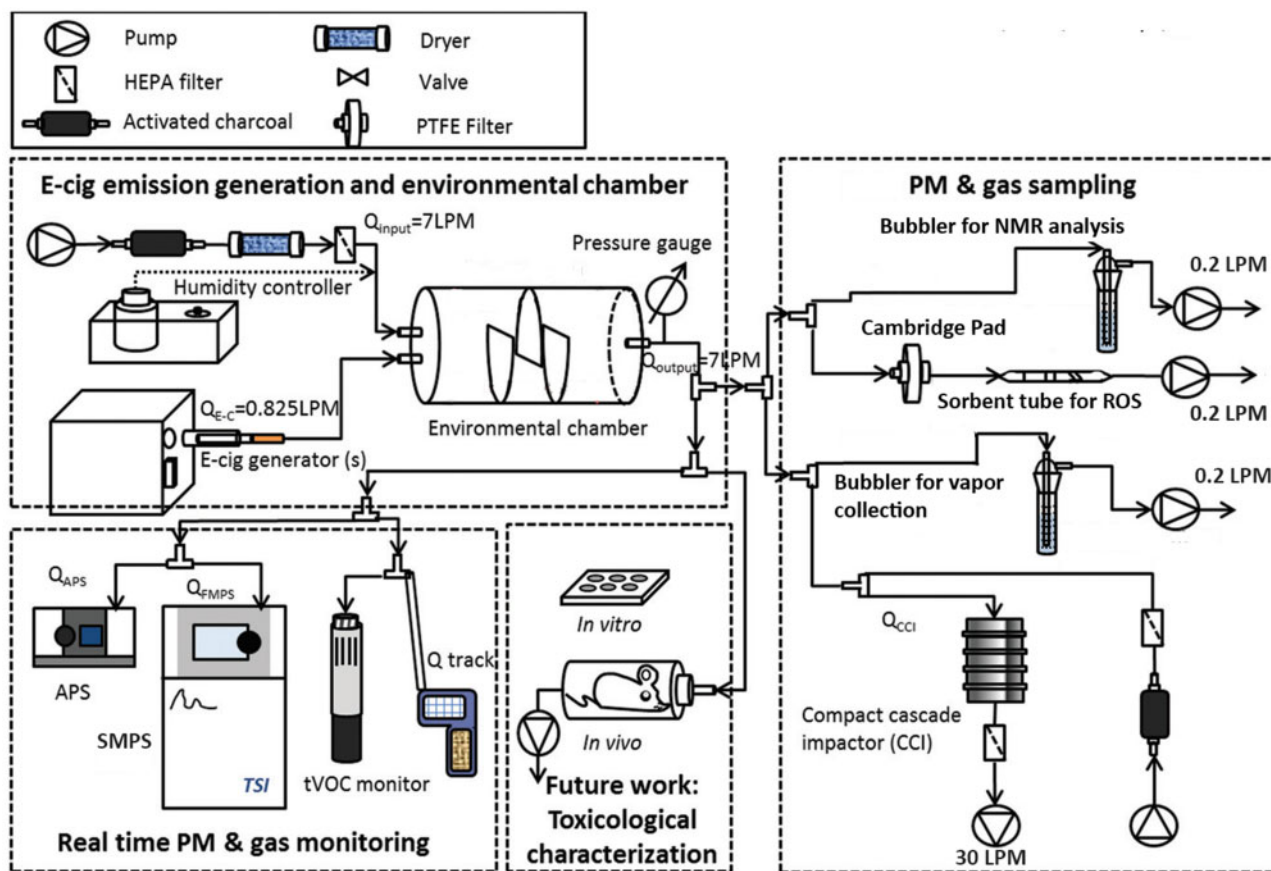


Figure 1. Schematic of the E-cig-Exposure Generation System (E-cig-EGS). E-cig-EGS (adapted from Zhao et al., 2016) for the generation, monitoring, sampling, and detailed physicochemical and toxicological characterization of real-world e-cig emissions.

and the cell surface area. For more details on the cellular exposure dose calculations, please refer to the [Supplementary Information](#).

Cell Viability Assay

Lactate dehydrogenase (LDH) released in the supernatant of Calu-3 and THP-1 cells treated for 24 h in a 96-well plate was used to assess the cell viability and measured using the Pierce LDH assay kit (cat. no. 88953, ThermoFisher Scientific, Waltham, Massachusetts) according to manufacturer's instructions. The absorbance was measured spectrophotometrically at a wavelength of 490 and 680 nm. Percent cytotoxicity was calculated by normalizing LDH activity of the treatments based on the maximum activity induced by the positive control, as described previously (Singh et al., 2022).

Metabolic Activity Assay

PrestoBlue HS cell viability reagent (cat. no. P50201, ThermoFisher Scientific) was used according to the manufacturer's instructions to assess the cellular metabolic activity. Fluorescence was measured at 560 nm (excitation)/590 nm (emission). Percent metabolic activity was normalized to the response from the negative control (untreated cells) assigned as 100%, as described previously (Singh et al., 2022).

Oxidative Stress/Reactive Oxygen Species Assay

ROS analysis was performed after 6 h treatment in a 96-well plate, using CellROX green reagent (cat. no. C10444, ThermoFisher-Scientific) according to the manufacturer's

instructions. Fluorescence was measured at 480 nm (excitation)/520 nm (emission). Percent ROS generation was normalized to the maximum ROS generation induced by the positive control assigned as 100%, as published previously (Singh et al., 2022).

Mitochondrial Membrane Potential Assay

Mitochondrial membrane potential ($\Delta\Psi_m$) was measured after 24 h treatment of Calu-3, using JC-1 Mitochondrial Membrane Potential Detection Kit (cat. no. 30001, Biotium Inc., Fremont, California), according to the manufacturer's instructions. Calu-3 cells were exposed in a 96-well plate containing 100 μ l/well of cell culture medium. Cells treated with carbonyl cyanide 3-chlorophenylhydrazone 0.1 mM for 30 min at 37°C were used as a positive control. Briefly, after 24 h exposure, the cell culture medium was removed, replaced with 100 μ l of JC-1 reagent working solution, and plates were incubated in a 37°C cell culture incubator for 15 min. The supernatant was removed, and cells were then washed once with 200 μ l PBS. Red and green fluorescence were measured at 550 nm (excitation)/660 nm (emission), and 485 nm (excitation)/535 nm (emission), respectively, using a fluorescence microplate reader. To calculate the $\Delta\Psi_m$, the ratio of red/green fluorescence was measured: the ratio is decreased in dead and apoptotic cells compared with healthy cells. Percent $\Delta\Psi_m$ was normalized to the response from the negative control (untreated cells) assigned as 100%.

Caspase-3 Activation Assay

Caspase-3 DEVD-R110 Fluorometric HTS Assay Kit (Biotium Inc., Fremont, California) was used to detect the activation of

Caspase-3 in treated Calu-3 cells, according to the manufacturer's instructions. Calu-3 cells were exposed in a 96-well plate containing 100 μ l/well of cell culture medium. Cells treated with staurosporine 2 μ M for 2 h at 37°C were used as a positive control. Briefly, after 24 h exposure, 100 μ l/well of assay buffer, containing enzyme-substrate (acDEVD)₂ R110 (2 mM) and cell lysis/assay buffer at a ratio of 50 μ l substrate per 1 ml buffer, was added to each well, the plate was incubated for 30 min and fluorescence was measured at 470 nm (excitation)/520 nm (emission). Percent caspase-3 activation was normalized to the response from the negative control (untreated cells) assigned as 100%.

Inflammatory Response Assessment

The supernatants from Calu-3 cells exposed to the higher dose representative of 257 puffs/m² (3 months) were collected after 24 h exposure and shipped in dry ice for cytokine and chemokine assessment using the Human Cytokine Array/Chemokine Array 48-Plex (HD48) assay (Eve Technologies, Calgary, Alberta). The samples were prepared according to Eve Technologies protocol, as previously described (Singh et al., 2022). The total concentration of cytokines/chemokines released was normalized to the number of cells and the negative control.

Statistical Analysis

The real-time aerosol characteristics (PNC and size distributions) were averaged across the consecutive measurements collected after reaching a steady state. Aerosol data analysis was performed in the TSI Aerosol Instrument Manager Software (AIM, v9.0) and average PNC and relevant aerosol size statistics (median, mode, geometric mean, and geometric standard deviation) were reported for each vaping atmosphere. All the cellular experiments were performed using 3 independent biological samples and each test was conducted in 3 technical triplicates.

Statistical analyses for all real-time and toxicological data were performed on GraphPad Prism using 2-way ANOVA tests and corrected for multiple comparisons: Dunnett's test was used to compare e-cig liquid composition versus baseline (Δ^8 THC 80%/VEA 20% for real-time data or negative/positive control for toxicological data); Sidak's test was used to compare 3.7 versus 5 V for real-time data and 85 versus 257 puffs/m² (1 vs 3 months) for toxicological data.

RESULTS

Real-Time Characterization of Released Aerosol PM

Figure 2 and Supplementary Figure 2 show the aerosol PNC as a function of size (in the nano to micron regime) in the e-cig aerosol generated from Δ^8 THC/VEA- and nicotine-based e-cigs, respectively, after reaching steady-state condition (approximately 1 min after initiation of the puffing protocol, irrespective of e-liquid type or operational voltage). Supplementary Table 2 summarizes the tPNC and the mean and modal aerosol sizes (along with standard deviations) at steady state during the e-cig aerosol generation from each e-liquid composition at the specified operational voltage, as measured using the APS (aerodynamic diameter range 0.5–20 μ m) and SMPS (mobility diameter range 10–420 nm) instrumentation. In more detail in the following sections.

Δ^8 THC/VEA-Based E-Liquids

For the 4 different Δ^8 THC/VEA e-liquid compositions (corresponding to VEA 0%–27%–54%–100%), the nano-PNC in the

e-cig aerosol varied (between 4.7×10^6 and 8.6×10^6 particles/cm³) across the 2 operational voltage, and the mean aerosol MPD ranged between 115 and 212 nm (Figure 2 and Supplementary Table 2). The micro-PNC was between 3364 and 7865 particles/cm³, whereas the mean APD remained between 1.25 and 1.43 μ m.

Effect of e-liquid composition. The tPNC for both size ranges was sensitive to e-liquid composition (ie, VEA concentration), without any apparent specific trend (Figure 2 and Supplementary Figure 2). For instance, at operational voltage 3.7 V, increasing the e-liquid VEA concentration from 0% to 27% raised the nano-PNC (from 5.9×10^6 to 7.7×10^6 particles/cm³), followed by decrease to 5.3×10^6 particles/cm³ at VEA 54% and subsequent increase to 7.0×10^6 particles/cm³ at VEA 100%. Similarly, the micro-PNC initially decreased from 4076 particles/cm³ at VEA 0% to 3364 particles/cm³ at VEA 27%, subsequently increased to 7414 particles/cm³ at VEA 54% and marginally decreased to 6982 particles/cm³ at VEA 100%. Similar fluctuations in PNC with e-liquid composition were also observed at the higher operational voltage 5 V: the nano-PNC steadily increased with increasing VEA concentration, starting from 4.7×10^6 particles/cm³ at VEA 27%, to 6.3×10^6 particles/cm³ at VEA 54%, and finally 8.6×10^6 particles/cm³ at VEA 100%. At the same voltage, the micro-PNC initially climbed from 6836 particles/cm³ at VEA 27% to 7856 particles/cm³ at VEA 54%, but then declined significantly to 3783 particles/cm³ at VEA 100%. The VEA concentration's effect on the average nanoparticle size was also apparent for both operational voltages, whereas the micron-sized particle number-size distributions remained relatively similar across the different compositions (Supplementary Figure 3). For instance, at 3.7 V, the e-liquid with VEA 27% had a significantly different nanoparticle size distribution (mean MPD: 126 nm) compared with the other compositions (mean MPD: 183–212 nm). At 5 V, the e-liquid with VEA 100% differed significantly (mean MPD: 115 nm) from the remaining compositions (mean MPD: 186–200 nm).

Effect of operating voltage. As is evident from Figure 2, the PNC for both size ranges and the nanoparticle size distribution (10–420 nm) were also dependent on the operational voltage utilized. Increasing operational voltage from 3.7 to 5 V increased the nano-PNC for e-liquids with VEA 54% (from 5.3×10^6 to 6.3×10^6 particles/cm³) and VEA 100% (from 7.0×10^6 to 8.6×10^6 particles/cm³) but decreased for VEA 27% (from 7.7×10^6 to 4.7×10^6 particles/cm³). Similarly, the voltage increase raised micro-PNC for VEA 27% (from 3364 to 6836 particles/cm³) and VEA 54% (from 7414 to 7856 particles/cm³), but significantly reduced them for VEA 100% (from 6982 to 3783 particles/cm³). The nanoparticle number-size distribution remained relatively the same across the 2 operational voltages for VEA 54% composition (mean MPD: 183–200 nm) but significantly shifted for the VEA 27% and VEA 100% compositions with operational voltage change. For VEA 27%, the nanoparticle size distribution shifted toward larger sizes at the higher voltage (mean MPD: from 126 nm at 3.7 V to 186 nm at 5 V), whereas for VEA 100%, it shifted toward smaller sizes with the increase in voltage (mean MPD: from 193 nm at 3.7 V to 115 nm at 5 V).

Nicotine-Based E-Liquids

For the 3 different nicotine-based e-liquid compositions (corresponding to Nic 2%–5%, Nic 5% + Menthol 2%), the released nano-PNC was in the range of $(5.2\text{--}9.2) \times 10^6$ particles/cm³ and the mean MPD remained between 110 and 125 nm, across the

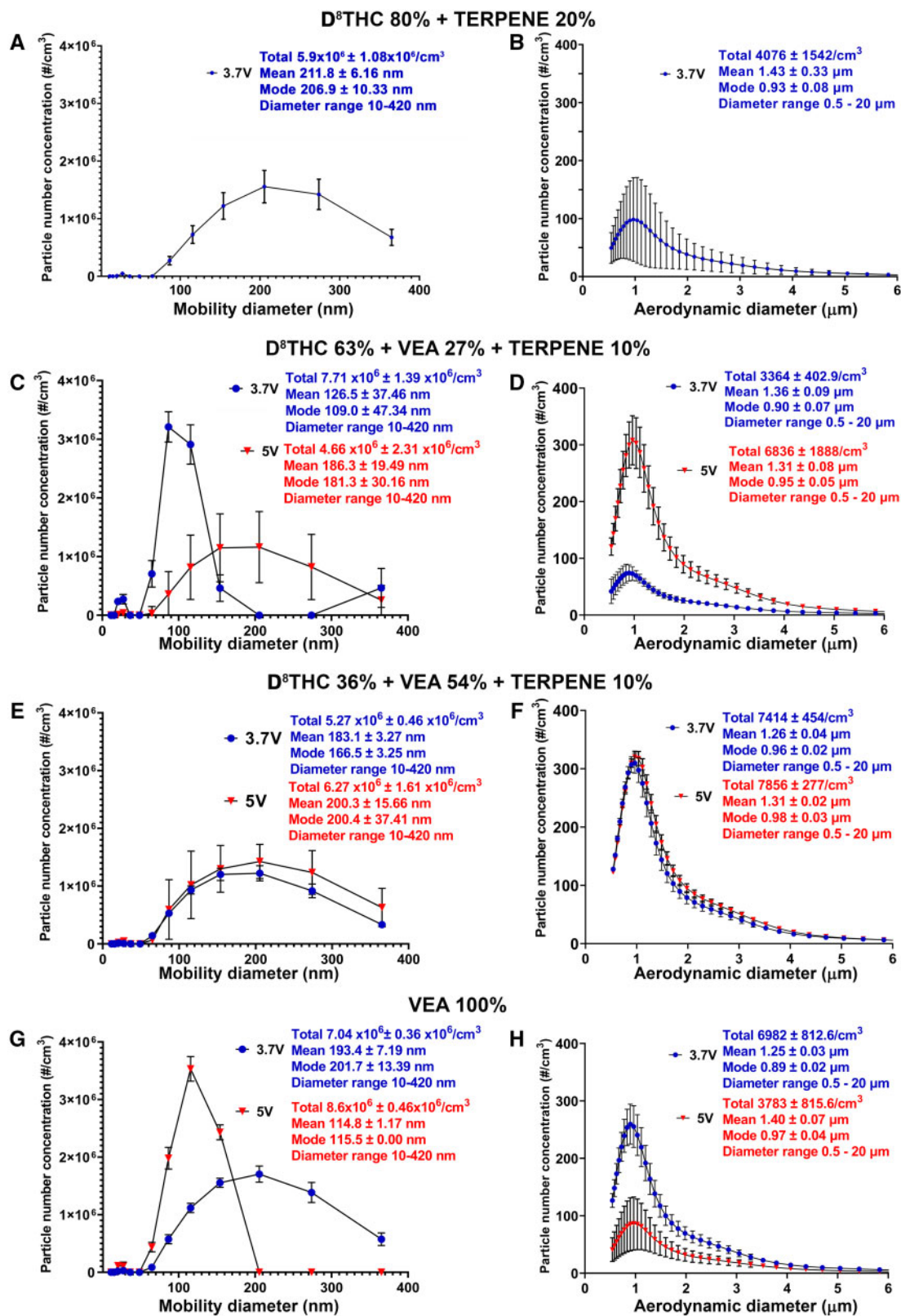


Figure 2. The total article number concentration and size distribution depend on both e-liquid composition and operational voltage. Comparison of number concentration, mean, and mode of particles generated from the 4 different THC-based e-liquid combinations, generated at 3.7 versus 5V. (A, C, E, G) mobility diameter range of 10–420 nm; (B, D, F, H) aerodynamic diameter range of 0.5–20 µm. Aerosol measurements were taken every 60 s for a period of 10 min for both APS and SMPS, and then the average of the consecutive readings of particle number concentration and mean/modal aerosol size was calculated. Thus the N was at least 10 for both measurements.

2 operational voltages (Supplementary Figure 2 and Table 2). The micro-PNC varied between 4052 and 7048 particles/cm³, and the mean APD remained relatively constant in the range of 1.25–1.31 μm.

Effect of e-liquid composition. Both the nano- and micro-tPNC were affected by the nicotine/menthol content in the e-liquid for a given operational voltage, whereas the aerosol size distribution and the mean aerosol size in both size regimes remained relatively the same across the different compositions (Supplementary Figs. 2 and 4). At operational voltage 3.7 V, the nano-PNC marginally decreased with nicotine content increase, from 9.2×10^6 particles/cm³ at Nic 2% to 8.6×10^6 particles/cm³ at Nic 5%, whereas the micro-PNC increased from 6178 to 6890 particles/cm³. The addition of menthol 2% to Nic 5% e-liquid (same voltage) further decreased both the nano-PNC to 6.4×10^6 particles/cm³ and the micro-PNC to 4052 particles/cm³.

Effect of operating voltage. The effect of operational voltage (3.7 vs 5 V) was assessed for one of the nicotine-based e-liquids (Nic 5% + menthol 2%). Both nano- and micron-PNC were sensitive to operational voltage utilized, but not the aerosol number-size distributions (Supplementary Figure 2). Nano-PNC decreased slightly with increasing operational voltage, from 6.4×10^6 particles/cm³ at 3.7 V to 5.2×10^6 particles/cm³ at 5 V, whereas micro-PNC rose steeply from 4052 particles/cm³ at 3.7 V to 7048 particles/cm³ at 5 V.

Real-Time Monitoring of Released Gaseous VOCs

Figures 3A–C show the real-time evolution of the total gaseous VOCs' concentration (tVOCs, ppm levels) released in the e-cig aerosol for all the different vaping atmospheres generated, for the first 10 min after the start of the puffing protocol. The concentration of tVOCs increased linearly or exponentially (sigmoidal or S-shaped growth curve) with time, depending on the e-liquid composition and the operational voltage. In more detail in the following sections.

Δ⁸THC/VEA-Based E-Liquids

The maximum tVOC concentration observed at the end of 10 min varied widely between the various vaping atmospheres generated from Δ⁸THC/VEA-based e-cigs (range: 0.173–24.5 ppm), depending on both e-liquids VEA concentration and operational voltage (Figs. 3A and 3B).

Effect of e-liquid composition. VEA concentration significantly affected the peak tVOC concentration for a given operational voltage, but without a definite correlation. At 3.7 V, the maximum tVOC concentration was achieved by VEA 27% (3.1 ppm), followed by VEA 0% (0.638 ppm), VEA 100% (0.327 ppm), and VEA 54% (0.173 ppm). At 5 V, the e-liquid with the highest tVOC concentration was VEA 100% (24.5 ppm), followed by VEA 27% (3.5 ppm) and VEA 54% (1.5 ppm).

Effect of operating voltage. Increasing the operational voltage from 3.7 to 5 V seemed to affect the tVOC evolution curve over time and increase the peak released tVOC concentration for all e-liquid compositions. Whereas the tVOC growth curve mostly remained linear at 3.7 V, it was exponential with a sigmoidal growth at 5 V with concentrations plateauing close to the 10-min mark. The most dramatic rise in tVOC concentration with the voltage increase was observed for VEA 100% (from 0.327 to 24.5 ppm, 75-fold increase), followed by VEA 54% (from 0.173 to

1.5 ppm, 9-fold increase), and VEA 27% (from 3.1 to 3.5 ppm, 1.1-fold increase).

Nicotine-Based E-Liquids

The peak tVOC concentration released in nicotine-based vaping atmospheres ranged between 0.044 and 0.707 ppm (Figure 3C), overall lower than Δ⁸THC/VEA-based e-liquids. The composition of nicotine did not affect the peak tVOC concentration (Nic 2%: 0.196 ppm vs Nic 5%: 0.044 ppm), whereas the addition of menthol flavoring significantly raised the tVOC concentration (Nic 5% + menthol 2%: 0.707 ppm vs Nic 5%: 0.044 ppm, 16-fold increase). Increasing the operational voltage from 3.7 to 5 V did not significantly alter the tVOC concentration released from the Nic 5% + menthol 2% e-cig (0.707–0.674 ppm, respectively).

Real-Time Monitoring of Released CO₂ and CO

Figures 3D–G show the bar graph concentration (in ppm levels) of CO₂ (D–E) and CO (F–G) released in the e-cig aerosol across the different vaping atmospheres, averaged for the first 10 min after the start of the puffing protocol. In more detail in the following sections.

Δ⁸THC/VEA-Based E-Liquids

The average released CO₂ level varied between 650 and 925 ppm (Figure 3D), whereas the average CO level ranged from negligible levels to 46 ppm (Figure 3F). The release of both CO₂ and CO was significantly affected by the e-liquid composition as well as the operational voltage, with more dramatic effects observed for CO levels with changes in composition and voltage.

Effect of e-liquid composition. The CO₂ level significantly increased initially in a dose-dependent manner with the increase in VEA concentration (VEA 0%: 723 ppm, VEA 27%: 779 ppm, VEA 54%: 876 ppm, $p < .0001$ vs VEA 0%), but then significantly decreased to 681 ppm ($p < .0001$ vs VEA 0%) at VEA 100%, when the e-cig was operated at 3.7 V (Figure 3D). Similarly, at the operating voltage of 5 V, the CO₂ level augmented from VEA 27% (862 ppm) to VEA 54% (925 ppm) ($p < .0001$ vs VEA 0%) and then declined to 650 ppm at VEA 100% ($p < .0001$ vs VEA 0%). The effect of VEA concentration on CO levels was quite pronounced at operational voltage 5 V (Figure 3F). Although the e-liquids VEA 0% and VEA 54% released negligible levels of CO, VEA 27% exhibited an average CO level of 10 ppm (peak: 35 ppm) ($p < .05$ vs VEA 0%) and VEA 100% showed the highest average CO level at 46 ppm (peak: 62 ppm) ($p < .0001$ vs VEA 0%).

Effect of operational voltage. Increasing the voltage from 3.7 to 5 V significantly increased the released CO₂ levels for VEA 27% (from 779 to 862 ppm, $p < .0001$) and VEA 54% (from 876 to 925 ppm $p < .0001$) e-liquids but suppressed the CO₂ levels for VEA 100% (from 681 to 650 ppm $p < .0001$) (Figure 3D). The CO levels increased tremendously with the operational voltage increase for VEA 27% (from negligible level to 10 ppm average, $p < .05$) and VEA 100% (from negligible level to 46 ppm average, $p < .0001$) but were unaffected for the VEA 0% and VEA 54% compositions where they remained negligible at both voltages (Figure 3F).

Nicotine-Based E-Liquids

The average CO₂ levels released from nicotine-based e-cigs remained relatively similar (approximately 900 ppm) across the different nicotine/menthol concentrations and voltage

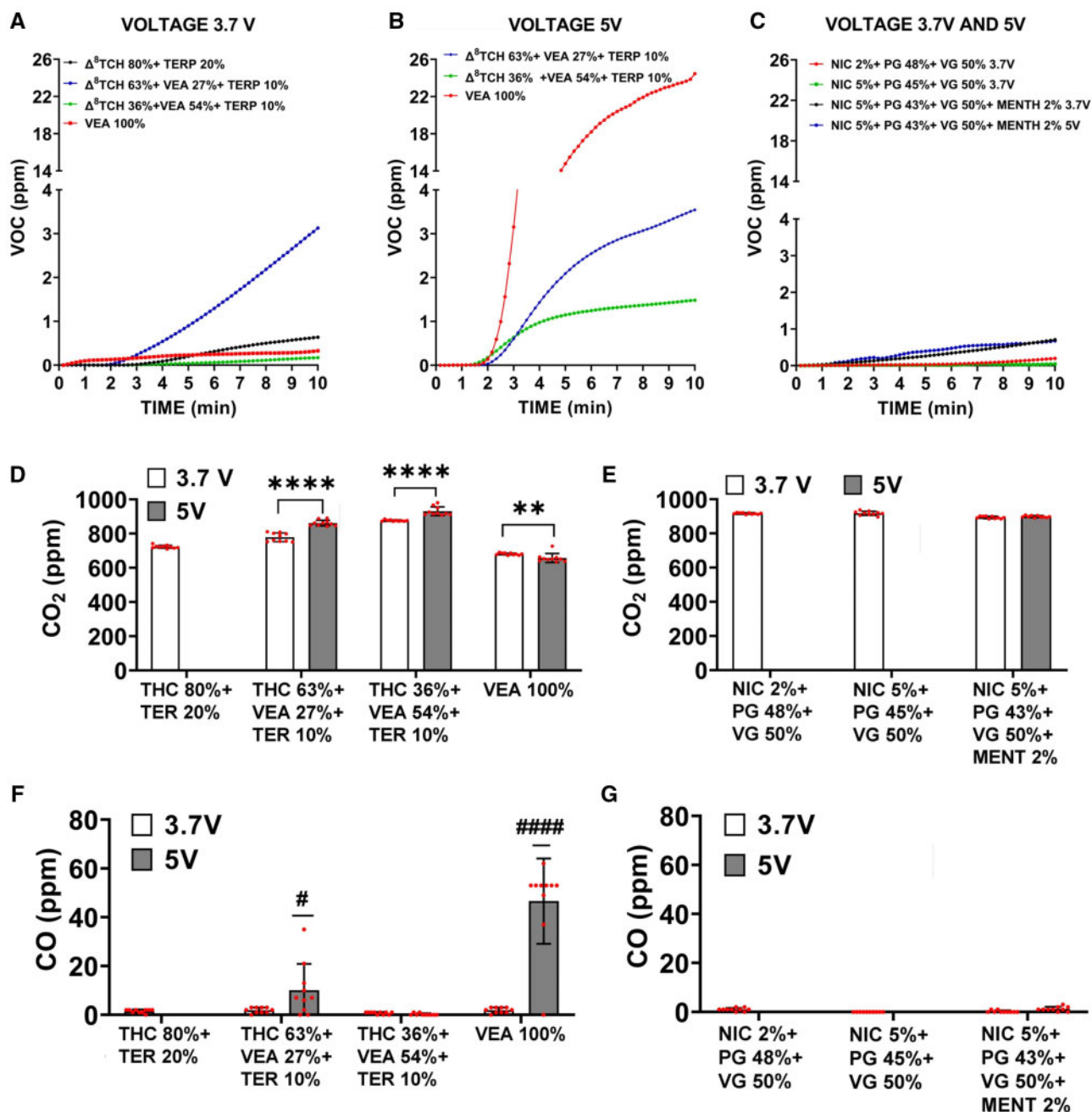


Figure 3. The emission of gaseous pollutants (VOC, CO₂, and CO) depends on both e-liquid composition and operational voltage. E-cig gaseous pollutants generation from different e-liquid combinations and under different operating voltages. A–C, Total VOC monitored for 10 min by tVOC monitor. D, E, CO₂ generation monitored for 30 min by Qtrak. F, G, CO generation monitored for 30 min by Qtrak. The measurement of VOC, CO₂, and CO were recorded only for the conditions listed in [Supplementary Table 1](#), therefore only 4 e-liquid compositions were examined at both voltages 3.7 and 5 V. All values are represented as the mean \pm SE. * $p < .05$, values statistically different between 2 voltages. Measurements were taken every 60 s for a period of 10 min, thus $N = 10$.

conditions, whereas the CO concentrations did not reach detectable levels for any of the nicotine atmospheres.

various vaping atmospheres. In more detail in the following sections.

Time-Integrated Mass-Size Distribution of Sampled Aerosol PM

[Supplementary Table 3](#) and [Figure 5](#) present the average PM mass concentration data (in units of mg/m^3) over the sampling period of the size-fractionated and collected aerosol particles in 3 size fractions ($\text{PM}_{0.1}$, $\text{PM}_{0.1-2.5}$, $\text{PM}_{>2.5}$) generated from the

Δ^8 THC/VEA-Based E-Liquids

The total PM mass concentration (across the 3 size fractions) released from the different Δ^8 THC/VEA e-liquids ranged widely between 67 and 910 mg/m^3 , depending on e-liquid VEA concentration and operational voltage. The bulk of the PM mass (94–99 wt%) was distributed between the $\text{PM}_{0.1}$ (11–60 wt%) and $\text{PM}_{0.1-2.5}$ (38–88 wt%)

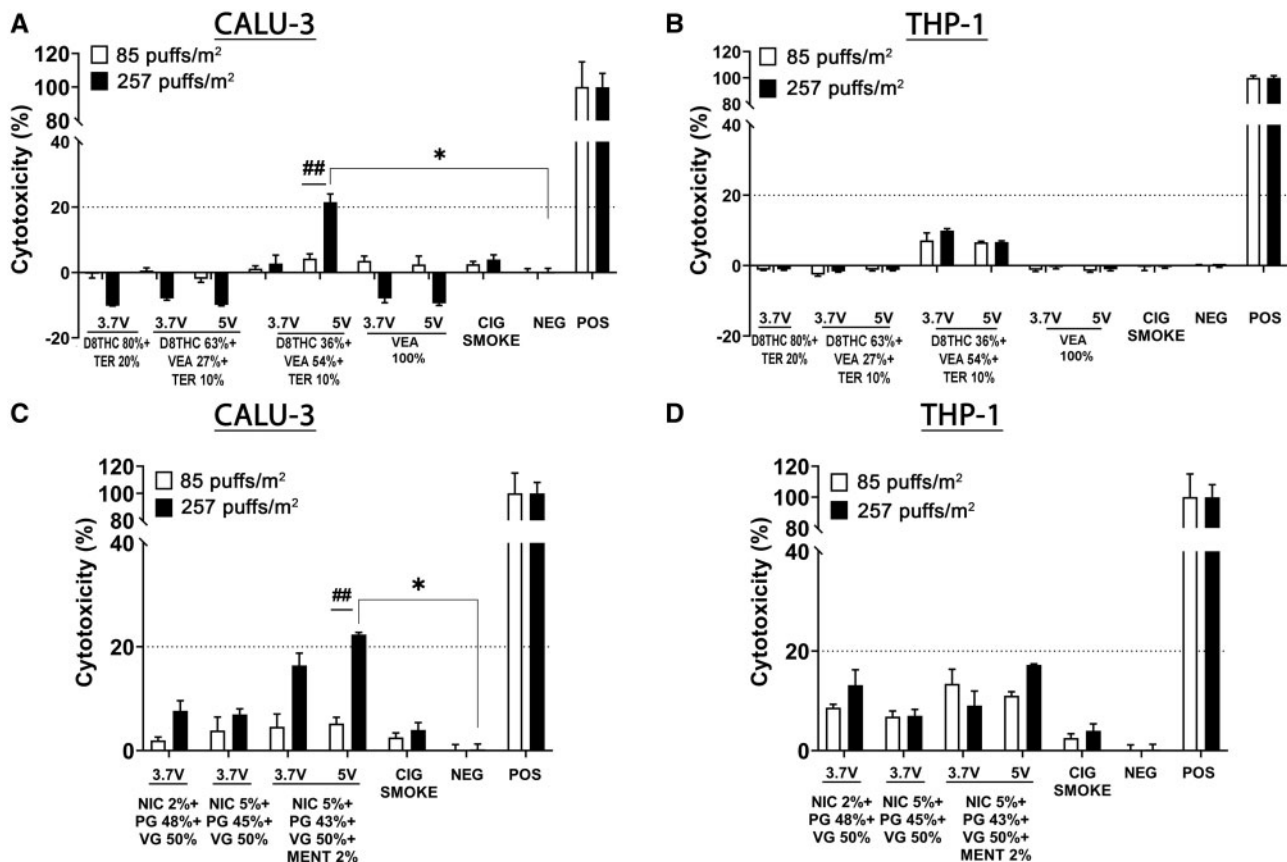


Figure 4. Cell viability was affected by the presence of VEA in Δ^8 THC and menthol flavoring in nicotine-based e-liquids especially at 5V. Acute *in vitro* cell viability assessment, using LDH assay, following exposure to e-cigs aerosols generated from different concentrations of THC/VEA or nicotine-based e-liquids, under 2 operational voltages (3.7 or 5 V), or cigarette smoke, at 2 doses of 85 and 257 puffs/m² (1 and 3 months), on human lung epithelial cells (Calu-3) (A, C) and peripheral monocytes (THP-1) (B, D). All values are represented as the mean \pm SE. * $p < .05$, values statistically different from untreated cells. # $p < .05$, values statistically different between 2 doses. Statistical analysis was performed on an average of 3 independent biological samples; fold changes $>20\%$ were deemed to be statistically significant ($p < .05$).

size fractions for all Δ^8 THC/VEA atmospheres, whereas the PM_{>2.5} size fraction constituted 1–6 wt% of the total PM mass.

Effect of e-liquid composition and operating voltage. The released total PM mass concentration significantly increased with increasing e-liquid VEA concentration at both operational voltages. In addition, increasing the voltage from 3.7 to 5V dramatically raised the PM mass concentration for all Δ^8 THC/VEA e-liquids. At 3.7V, VEA 100% released the highest PM mass concentration (311 mg/m³) followed by VEA 54% (306 mg/m³), VEA 27% (114 mg/m³), and VEA 0% (67 mg/m³). A similar trend was observed at 5V along with tremendously increased PM mass concentrations for each e-liquid compared with 3.7V (VEA 100%: 910 mg/m³, VEA 54%: 447 mg/m³, VEA 27%: 245 mg/m³).

Nicotine-Based E-Liquids

The total PM mass concentration released in the different nicotine-based vaping atmospheres ranged from 240 to 668 mg/m³, with the majority of the PM mass lying in the PM_{0.1–2.5} size fraction (82–87 wt%), followed by PM_{0.1} (11–16 wt%) and PM_{>2.5} (1–2 wt%) size fractions. Increasing nicotine content in e-liquid significantly raised the PM mass concentration, from 300 mg/m³ (Nic 2%) to 417 mg/m³ (Nic 5%) at operational voltage 3.7V. Furthermore, adding menthol 2% flavoring to the Nic 5% e-liquid further increased the PM concentration to 668 mg/m³, at the same voltage. However, at the higher operational voltage of 5V,

the PM concentration from the Nic 5% + menthol 2% e-liquid significantly declined to 240 mg/m³.

Cytotoxicity of E-Cig Emissions

In this section, we present the results for the acute *in vitro* cytotoxicity assessment of the generated and sampled e-cig aerosols from the different e-liquid compositions under the investigated voltage conditions for both Calu-3 and THP-1 cell lines.

Cell Viability (LDH and PrestoBlue Assays)

Figure 4 shows the results for the LDH release after 24 h from Calu-3 human lung epithelial cells (Figs. 4A and 4C for Δ^8 THC/VEA- and nicotine-based e-liquids, respectively) and THP-1 human monocyte cell line (Figs. 4B and 4D for Δ^8 THC/VEA- and nicotine-based e-liquids, respectively), exposed to 2 doses of e-cig aerosol corresponding to 85 and 257 puffs/m² (1 and 3 months). Neither of the e-cig aerosol samples induced significant LDH release in both cell lines, except for the higher dose (257 puffs/m², 3 months) of aerosol produced from VEA 54% at 5V and Nic 5% + menthol 2% at 5V that induced a slight but significant increase of LDH release after 24 h ($>20\%$, $p < .05$) in the Calu-3 cells (Figs. 4A and 4C).

An indirect method to measure cell viability is the cells' metabolic activity. After 24 h exposure of Calu-3 to both concentrations of aerosols, the metabolic activity did not decrease significantly. However, similar to the LDH release, aerosols emitted from VEA

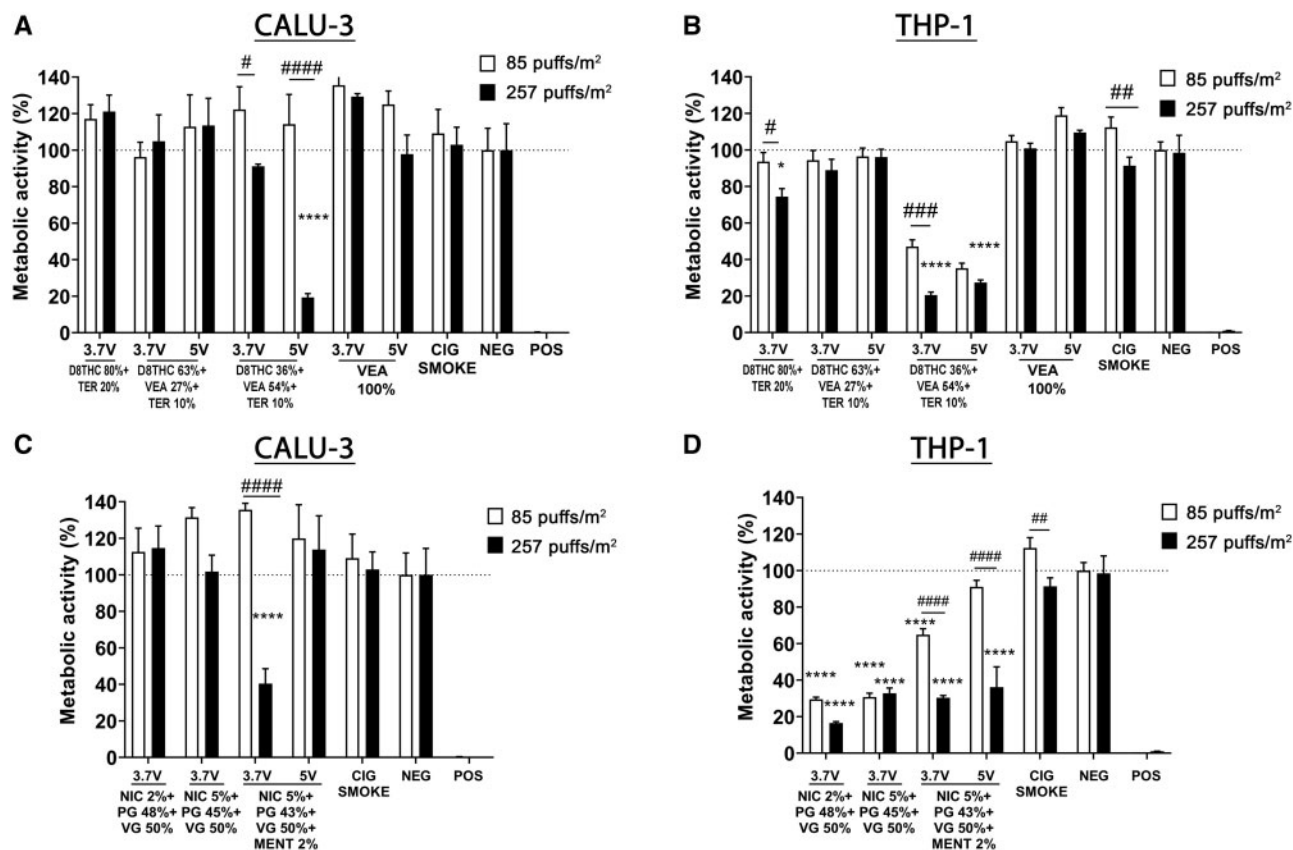


Figure 5. Alterations in metabolic activity in Calu-3 and THP-1 cell lines are dependent on e-cigs e-liquid composition and operational voltage. Acute *in vitro* cytotoxicity assessment through cells metabolic activity, using Presto blue assay, following exposure to e-cigs aerosols generated from different concentrations of THC/VEA- or nicotine-based e-liquids, under 2 operational voltages (3.7 or 5 V), or cigarette smoke, at 2 doses of 85 and 257 puffs/m² (1 and 3 months), on human lung epithelial cells (Calu-3) (A, C) and peripheral monocytes (THP-1) (B, D). All values are represented as the mean \pm SE. * $p < .05$, ** $p < .01$, *** $p < .001$, **** $p < .0001$ compared with negative control. # $p < .05$, ## $p < .01$, ### $p < .001$, #### $p < .0001$ compare between 2 doses. Statistical analysis was performed on an average of 3 independent biological samples; fold-changes $>20\%$ were deemed to be statistically significant ($p < .05$).

54% (5V) and nicotine 5%+ menthol 2% (3.7V) induced a significant and dose-dependent reduction of metabolic activity in Calu-3 epithelial cells (**** $p < .0001$ compared with negative control, #### $p < .0001$ higher dose vs lower dose) (Figs. 5A and 5C).

Similar to Calu-3 epithelial cells, THP-1 monocyte cells experienced a statistically significant dose-dependent diminution in metabolic activity when exposed to both doses of VEA 54% aerosol generated at 3.7 or 5V (**** $p < .0001$) (Figure 5B). In addition, THP-1 cells exposed to both doses of nicotine-containing aerosols also showed a statistically significant decrease in metabolic activity (**** $p < .0001$), except for the lower dose of Nic 5% + menthol 2% (3.7V) (Figure 5D).

To better understand the cytotoxic effect of the aerosol generated from VEA 54% (5V), both cell lines were exposed to higher concentrations of the same aerosol, 1020, 510, 255, and 85 puffs/m², corresponding to 12-, 6-, 3-, and 1-month vaping periods (Supplementary Figure 6). Although Calu-3 epithelial cells did not exhibit any significant release of LDH or decrease in metabolic activity for any of the doses tested (Supplementary Figs. 6A and 6C), THP-1 monocytes showed a dose-dependent increase of LDH release compared with the negative control, and a decreasing metabolic activity only at 257 puffs/m² (3 months) (Supplementary Figs. 6B and 6D).

Cell ROS Production

Figure 6 shows the ROS generation from human lung epithelial cells (Calu-3) (Figs. 6A and 6C) and human monocyte cell line

(THP-1) (Figs. 6B and 6D), exposed to 2 doses of aerosols, corresponding to 85 and 257 puffs/m² (1 and 3 months). Aerosols generated from Δ^8 THC- or nicotine-containing e-liquids did not induce a significant generation of ROS in Calu-3 epithelial cells. Conversely, the THP-1 monocyte cells exposed to both doses of VEA 54% at 3.7 and 5V generated a significant amount of ROS in a dose-dependent manner (**** $p < .0001$) (Figure 6B). THP-1 monocyte cells exposed to both concentrations of aerosols from nicotine-based e-liquids also showed a dose-dependent generalized augmented production of ROS (**** $p < .0001$) (Figure 6D).

Apoptosis JC1: Caspase-3

To understand better the mechanism of cell damage, the alteration of mitochondrial membrane potential ($\Delta\Psi_m$) and the activation of caspase-3 were measured in Calu-3 epithelial cells. Overall, all the e-cig aerosols induced a dose-dependent loss in $\Delta\Psi_m$ and activation of caspase-3 (Figure 7). Specifically, in the Δ^8 THC group, the most significant mitochondrial perturbation was caused by both doses of VEA 27% at 5V (-50% and -60% for 85 and 257 puffs/m², respectively, **** $p < .0001$) and the high dose of VEA 54% at 3.7 and 5V (-60% and -50% respectively, **** $p < .0001$) (Figure 7A). Among the nicotine group, all the high doses induced a significant reduction of $\Delta\Psi_m$ (-50% , **** $p < .0001$), whereas the lower doses only induced a slight decrease in $\Delta\Psi_m$ (-20% , **** $p < .0001$) (Figure 7C).

The assessment of the caspase-3 activation showed that among the aerosols generated from Δ^8 THC-based e-liquids,

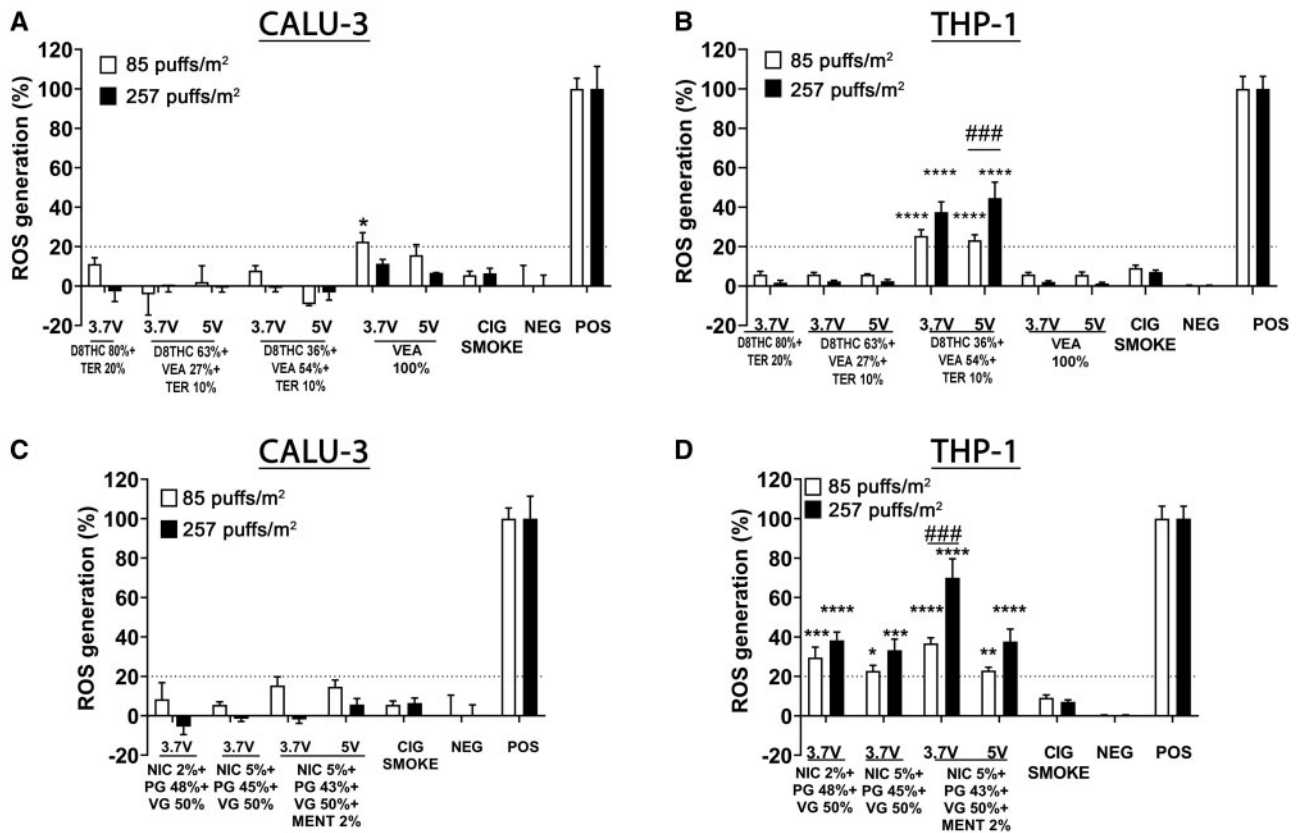


Figure 6. In THP-1 monocytes, but not in Calu-3 cells, VEA 54% (3.7 and 5 V) induced a significant and dose-dependent reactive oxygen species (ROS) generation. Acute *in vitro* assessment of ROS generation in human lung epithelial cells (Calu-3) (A, C) and peripheral monocytes (THP-1) (B, D) exposed for 24 h to aerosols generated from different concentrations of Δ^8 THC/VEA or nicotine-based e-liquids under 2 operational voltages (3.7 or 5 V), or cigarette smoke, at 2 doses of 85 and 257 puffs/m² (1 and 3 months). All values are represented as the mean \pm SE. * $p < .05$, ** $p < .01$, *** $p < .001$, **** $p < .0001$ compared with negative control. # $p < .05$, ## $p < .01$, ### $p < .001$, #### $p < .0001$ compare between 2 doses. Statistical analysis was performed on an average of 3 independent biological samples; fold changes $>20\%$ were deemed to be statistically significant ($p < .05$).

high doses of VEA 54% generated at both operational voltages (3.7 and 5 V) led to an increased caspase-3 activation (approximately 40%, **** $p < .0001$ compared with negative control) (Figure 7B). Aerosol generated from both doses of VEA 100% at 3.7 V and the high dose of VEA 100% at 5 V also significantly stimulated the activation of caspase-3 (3.7 V: approximately 40%, **** $p < .0001$; 5 V: approximately 30%, ** $p < .01$ compared with negative control), as well as cigarette smoke (approximately 30%, *** $p < .001$ compared with negative control) (Figure 7B). Among the cells treated with nicotine-based aerosols, the higher doses induced significant activation of caspase-3 (approximately 40%, **** $p < .0001$ compared with the negative control, except Nic 5% + PG 45% + VG 50% approximately 25% ** $p < .001$), whereas the lower dose had a very mild effect (approximately 20%, compared with negative control) (Figure 7D).

In Vitro Inflammatory Response

Figure 8 and Supplementary Table 4 show the analysis of the cytokines released in the supernatant of the lung epithelial cells exposed to the higher dose of e-cig emissions for 24 h. Δ^8 THC containing emissions induced a general suppression of pro- and anti-inflammatory markers, including sCDL40, EGF, Eotaxin, FTL-3L, Fractalkine, IFN- α 2, IFN- γ , IL-1 β , IL-2, -3, -5, -9, -10, -12p40, -12p70, -13, -17A, IL-17E/-25, -17F, -27, IP-10, MCP-3, PDGF-AA, TGF- α , and TNF- α .

In contrast with the general trend, the exposure to VEA 54% at both 3.7 and 5 V did not affect the secretion of IL-6, IL-15, and

MCP-1, whereas it induced upregulation of FGF-2 ($p < .01$ and $p < .0001$, respectively), G-CSF (both $p < .001$), IL-1 α (both $p < .0001$), IL-1RA ($p < .001$ and $p < .01$, respectively), IL-18 ($p < .05$ and $p < .001$, respectively), M-CSF (both $p < .001$), and PDGF-AB/BB ($p < .05$ and $p < .0001$, respectively) and downregulation of GRO- α (both $p < .0001$), IL-4 (both $p < .0001$), IL-22 (both $p < .0001$), MDC ($p < .001$ and $p < .01$, respectively), RANTES (both $p < .0001$), TNF- β (both $p < .0001$), and VEGF-A (both $p < .0001$) (Figure 8A). Δ^8 THC 80% + TER 20% only upregulated FGF-2 ($p < .01$), GRO α ($p < .05$); VEA 100% aerosol generate at 3.7 and 5 V upregulated FGF-2 ($p < .0001$, only 5 V), GRO- α (both $p < .0001$), IL-4 (only 3.7 V $p < .05$), whereas downregulated IL-6 ($p < .0001$ only 3.7 V), IL-15 ($p < .0001$), PDGF-AB/BB (both $p < .0001$) and RANTES ($p < .001$ and $p < .0001$, respectively). VEA 27% at 3.7 and 5 V also increased the release of FGF-2 (only at 3.7 V $p < .05$), GRO- α (both $p < .0001$), and MCP-1 ($p < .05$ at 5 V) (Figure 8A). The only cytokines that were not affected by any treatment were IL-8 and Gm-CSF (Figure 8A). IL-7, MIP-1, and MIP-3 were undetected (data not shown).

Similarly to aerosol generated by Δ^8 THC containing e-liquid, aerosols from the nicotine based e-liquids also suppressed the release of sCD40L, EGF, Eotaxin, FLT-3L, fractalkine, GRO- α , IFN- α 2, IFN- γ , IL-1 β , -2, -3, -4, -5, -9, -10, -12p40, -12p70, -13, -17A, 17E/IL-25, 17F, -22, -27, IP-10, MCP-3, MDC, MIG, MIP-1B, PDGF-AA, RANTES, TNF- α , TNF- β , VEGF-A, and stimulated the release of FGF-2, IL-1 α , IL-1RA, IL-18, and M-CSF. G-CSF, GM-CSF, IL-8, MCP-1, and PDGF-AB/BB were not affected by any nicotine e-cig aerosol. IL-7 and MIP-1A were not detected (Figure 8B).

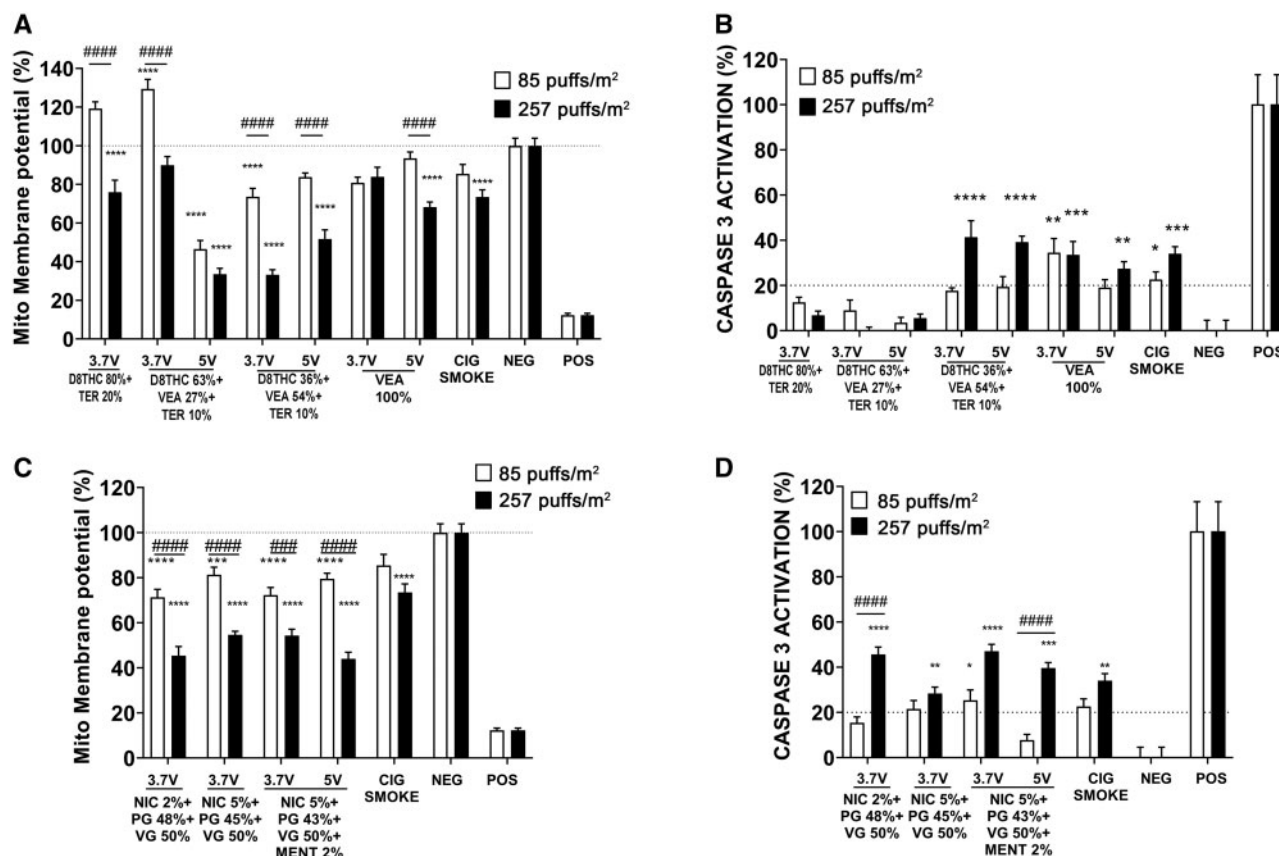


Figure 7. High doses of e-cigs aerosols induce the greater mitochondrial membrane potential ($\Delta\Psi_m$) alteration and caspase-3 activation in Calu-3 cells. Acute *in vitro* assessment of mitochondrial membrane depolarization and apoptosis, using JC-1 dye (A, C) and caspase-3 activation (B, D) in human lung epithelial cells (Calu-3) exposed for 24 h to aerosols generated from different concentrations of Δ^8 THC/VEA or nicotine-based e-cigs at 2 different voltages (3.7 or 5 V) or cigarette smoke, at 2 doses of 85 and 257 puffs/m² (1 and 3 months). All values are represented as the mean \pm SE. * $p < .05$, ** $p < .01$, *** $p < .001$, **** $p < .0001$ compared with negative control. # $p < .05$, ## $p < .01$, ### $p < .001$, #### $p < .0001$ compare between 2 doses. Statistical analysis was performed on an average of 3 independent biological samples; fold changes $>20\%$ were deemed to be statistically significant ($p < .05$).

The most bioactive emission was Nic 5% + menthol 2% generated at 3.7 V, which in addition to the aforementioned biomarkers, increased the release of IL-15 ($p < .001$) and TGF- α ($p < .0001$), and inhibited the secretion of IL-6 ($p < .01$) (Figure 8B). The aerosols released from Nic 2% also suppressed the release of IL-6 ($p < .05$) and MCP-1 ($p < .01$), whereas increasing the secretion of IL-15 ($p < .05$) (Figure 8B).

DISCUSSION

The main goal of our study was to investigate the physicochemical properties and potential cytotoxicity of aerosols generated from various concentrations and operational voltages of Δ^8 THC/VEA-based e-liquids, as they have been presumably associated with EVALI, due to their detection in the majority of patients' samples and vaping products (Blount *et al.*, 2020; Duffy *et al.*, 2020; FDA, 2020; Muthumalage *et al.*, 2020a; Taylor *et al.*, 2019), compared with conventional nicotine e-cigs.

Using a versatile E-cig-EGS, which enables the systematic generation of real-world e-cig exposures, and through the adjustment of operational parameters (such as e-cig brand/type, e-liquid composition, operating voltage, and puffing topography) (Zhao *et al.*, 2016, 2018a,b), this study tested combinations of Δ^8 THC, VEA, and terpenes at various concentrations derived from EVALI patients' products and compared them with the conventional MMP concentration (Δ^8 THC 80% + Terp 20%)

(Supplementary Table 1). Because a small proportion of patients reported only nicotine vaping, 4 different combinations of nicotine, diluents (PG: VG), and flavors (menthol) were also analyzed (Supplementary Table 1) as comparators. In addition, because the inspected EVALI cartridges showed burns and marks of high temperature, hence high operational voltage, the e-cigs containing only selected e-liquids combination were operated at 2 different voltages, 3.7 (low) and 5 V (high) (Supplementary Table 1).

Effect of E-Liquid Composition and Voltage on Particles' Physical Properties

We believe this study to be the first to provide a comprehensive and systematic physical characterization of particles and gases emitted by pyrolysis of Δ^8 THC + Terp with or without VEA in comparison with those of nicotine-based e-liquids.

The only previous study investigating the particle size distribution of aerosol generated from VEA e-liquid alone showed a variation of tPNC between 10^7 and 10^8 particles/cm³, with count median diameter (CMD) range 50–200 nm mostly depending on the puff flow rate and operational voltage: as the flow rate increased, the CMD decreased while the tPNC increased (Mikheev *et al.*, 2020). Although no data are available on the characterization of Δ^8 THC-based aerosols, the nicotine-based ones showed tPNC variation between 10^6 and 10^9 particles/cm³ (Fuoco *et al.*, 2014; Lamos *et al.*, 2019; Zhao *et al.*, 2016), with a CMD range of 24–450 nm (Ingebretsen *et al.*, 2012; Scungio *et al.*, 2018), and a

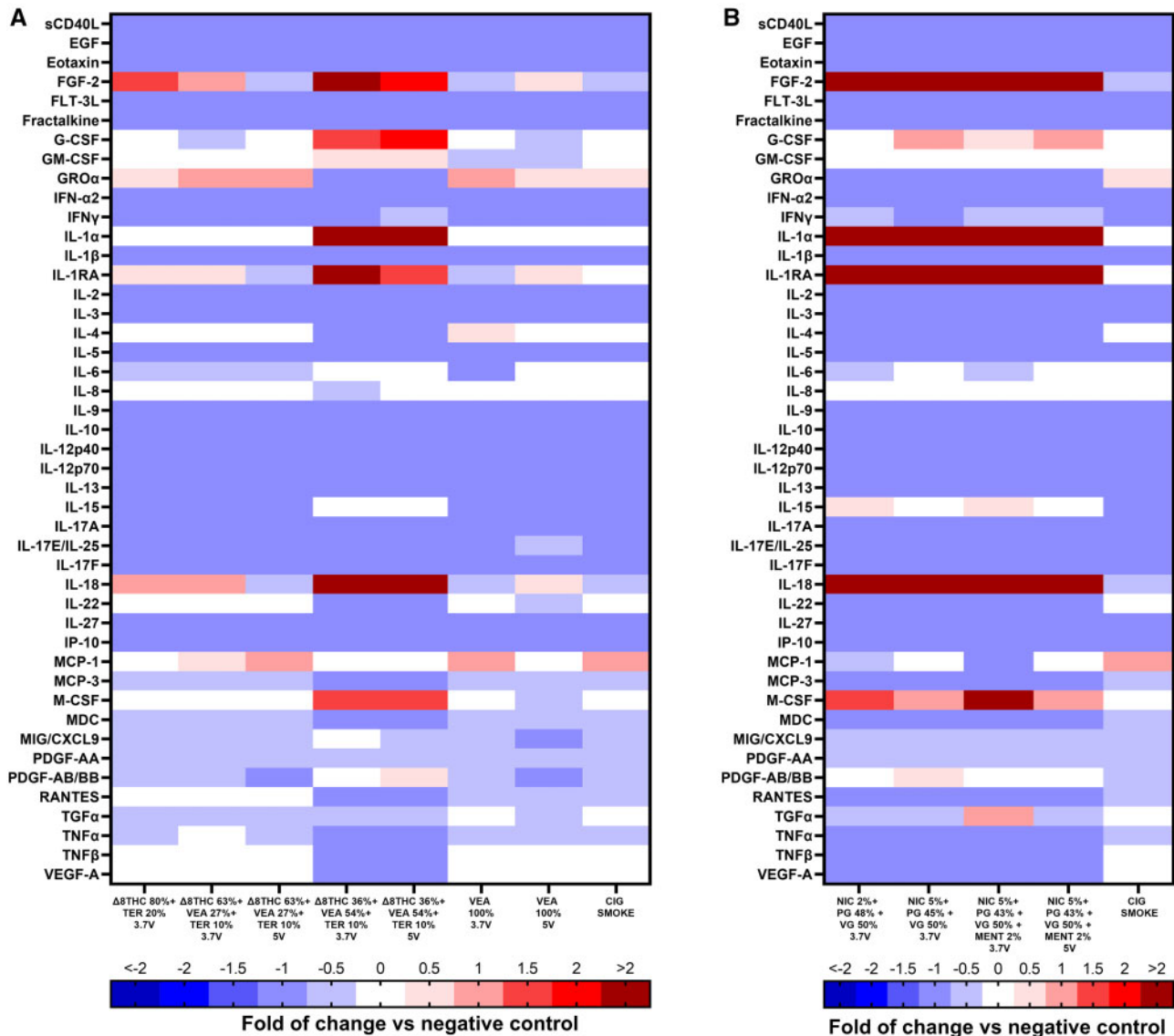


Figure 8. Aerosols generated from Δ^8 THC 36% + VEA 54% + Ter 10% and Nic 5% + menthol 2% are the most bioactive emission. Measured levels of cytokines and chemokines in the supernatant of Calu-3 exposed for 24 h to aerosols generated from different concentrations of Δ^8 THC/VEA or nicotine-based e-liquids at 2 different voltages (3.7 or 5 V) or cigarette smoke, at high dose of 257 puffs/m² (3 months). Statistical analysis was performed on an average of 3 biological samples. Values are presented as fold of change versus negative control (0). For the statistical analysis, please refer to the text or [Supplementary Table 4](#).

bimodal (Mikheev et al., 2016; Zhao et al., 2016) or unimodal (Fuoco et al., 2014; Zhang et al., 2013) size distribution, related to different puffing parameters, e-liquid compositions, and e-cigs devices. In agreement with our previous study (Zhao et al., 2016), real-time monitoring data revealed that tPNC emitted from both Δ^8 THC- and nicotine-based e-liquids was in the range of 10⁶ particles/cm³, and the majority of particles were <500 nm in size, with a single peak approximately 153 nm (coefficient of variation, CV, 27%). Thousands of particles/cm³ were reported in the size range 0.5–20 μ m with a single peak approximately 1.30 μ m (CV 5%) (Supplementary Table 2 and Figs. 2–5). The subtle variations in the aerosol mean size were e-liquid composition and voltage dependent, however, no significant differences in terms of tPNC or size distribution were noticed between conventional nicotine and Δ^8 THC aerosols, even in the presence of VEA.

Additionally, the variability in particle mass concentration across all the Δ^8 THC-based aerosols was in the range 66.61–

908.9 mg/m³, due to different e-liquid composition and voltage, where the lower and the higher amount were emitted by Δ^8 THC 80% + Terp 20% (3.7 V) and VEA 100% (5 V), respectively. Nicotine-based e-liquids generated PM with a mass concentration in the range 239.69–668.48 mg/m³, the minimum and maximum corresponding to Nic 5% + PG 43% + VG 50% + menthol 2% at 5 and 3.7 V, respectively.

Emissions from Δ^8 THC 36% + VEA 54% + Terp 10% or VEA 100% e-liquids show a PM mass-size distribution similar to the nicotine-based ones, whereas the PM mass concentrations were similar for the Δ^8 THC/VEA e-liquids (305.78–909.36 mg/m³) and nicotine-based ones (239.69–668.48 mg/m³). The larger mass concentration was reported for the PM_{0.1–2.5} size fraction regardless of the voltage. This is in agreement with our previous data published for nicotine-based e-liquids (Zhao et al., 2016, 2018a,b). In contrast, emissions from Δ^8 THC 80% + Terp 20% or Δ^8 THC 63% + VEA 27% + Terp 10% regardless of the voltage

showed a PM concentration (66.6–163.15 mg/m³) and size distribution more evenly distributed between PM_{0.1} and PM_{0.1–2.5} size fractions (Supplementary Table 3 and Figure 5). Such variations in the PM mass size distribution and concentration can be attributed to the differences in e-liquid composition and operating voltage.

Recently, Meehan-Atrash *et al.* investigated the tVOC emission from pure THC or THC/Terpenes 90:10 v/v, generated through 2 different methods, dabbing or CCell cartridges vaporizer, operated at 3 voltages: 3.2, 4.0, or 4.8 V. They reported that tVOCs increased in a voltage-dependent manner, across the 3 voltage vaping conditions (Meehan-Atrash *et al.*, 2019). In our study, tVOC, as well as CO₂ and CO, were also voltage- and e-liquid composition dependent without any specific pattern (Figure 3).

The concentration of CO₂ varied between 657 and 930 ppm within the Δ⁸THC group, whereas in the nicotine group varied between 893 and 918 ppm, in a voltage and e-liquid composition-dependent manner (Figure 3). In contrast, the CO concentration was negligible across all the Δ⁸THC and nicotine atmospheres, even though VEA 100% (5 V) and Δ⁸THC 63% + VEA 27% + Terp 10% (5 V) reached an average of 46 and 10 ppm, respectively (Figure 3). The World Health Organization (WHO) determined the time-weighted average exposure limits for some CO concentrations so that the carboxyhemoglobin level of 2.5% was not exceeded, consisting in 8 h for 9 ppm CO, 1 h for 26 ppm CO, and 30 min for 52 ppm CO. Hence, besides the fact that e-cigs containing only VEA are not available in the real-world, the combination Δ⁸THC 63% + VEA 27% + Terp 10% (5 V) releases the higher amount of CO only when the e-liquid is running out, and the temperature is consequently higher, therefore the average of 10 ppm would only apply to a few minutes of vaping and thus likely would not exceed the recommended limit for 8 h.

In summary, the tPNC, PM mass-size distribution, tVOC, and CO₂ levels for Δ⁸THC/VEA e-liquids exhibited a different trend compared with conventional nicotine-based ones, thus suggesting that multiple chemical reactions can take place in the pyrolysis of combinations of e-liquids at various operational voltages, which leads to the release of a mixture of chemicals.

Most likely, the chemical composition will be different as well across the 2 classes of e-liquids. Pyrolysis of the e-liquids is known to generate a complex mixture of organic chemicals and heavy metals, depending on the e-liquid composition and the temperature inside the cartridge which is driven by the applied voltage (Jiang *et al.*, 2020; Ko and Kim, 2022). It is well-known that combustion temperature can alter the size, number concentration, and chemical composition of emitted aerosols and the nature and concentration of gaseous byproducts (Geiss *et al.*, 2016; Ko and Kim, 2022; Lechasseur *et al.*, 2019; Zhao *et al.*, 2018a). This is evident in the case of VEA 100% where the higher voltage (5 V) induces an extremely high concentration of CO, VOC, and particle number/mass concentration compared with the other atmospheres, which is likely driven by the accelerated combustion of pure VEA at the higher temperature produced inside the cartridge. We are currently conducting a detailed chemical analysis of the sampled e-cig aerosols, and it will be reported in a future manuscript.

Effect of E-Liquid Composition and Voltage on Cytotoxicity and Inflammation

In vitro acute toxicological assessment of the emission from Δ⁸THC and nicotine-based e-liquids was conducted using human lung epithelial cells Calu-3 and human peripheral

monocytes THP-1. These cell lines were selected because the EVALI syndrome is characterized by a disruption of the alveolar epithelium, and because the alveolar macrophages represent the first line of defense against particles in the lungs. Both cell lines were exposed to 2 different concentrations of aerosols, 85 and 257 puffs/m², representative of 1 and 3 months vaping, to assess potential dose-response relationships and mimic the exposure necessary for the development of EVALI (Christiani, 2020; Layden *et al.*, 2020). Emissions from a conventional tobacco cigarette were used as a comparator.

The results showed that most of the emissions from Δ⁸THC/VEA and nicotine-based e-liquids did not affect viability, metabolic activity, and ROS generation of either Calu-3 epithelial cells or THP-1 monocytes (Figs. 4–6). The only exceptions were the higher dose of aerosol from Δ⁸THC 36% + VEA 54% + Terp 10% (5 V) and nicotine 5% + PG 43% + VG 50% + menthol 2% that induced a significant increase of LDH release (>20%, $p < .05$), and a reduction in metabolic activity ($p < .0001$) in Calu-3 epithelial cells (Figs. 4 and 5), and Δ⁸THC 36% + VEA 54% + Terp 10% (3.7 and 5 V) and nicotine-based aerosols, that induced a sharp and dose-dependent decrease in metabolic activity and increased ROS generation ($p < .0001$) in THP-1 monocytes, compared with cigarette smoke and control-treated cells (Figs. 5 and 6). Taken together, this data show that the most bioactive aerosol generated from the Δ⁸THC/VEA e-liquid group was Δ⁸THC 36% + VEA 54% + Terp 10% (5 V). However, the cytotoxicity did not increase in Calu-3 epithelial cells when they were challenged with increasing doses of the aerosol, up to 1020 puffs/m² (12 months), whereas a statistically significant dose-dependent release of LDH was recorded in THP-1 monocytes, accompanied by a decreased metabolic activity only after 257 puff/m² (3 months) dose exposure (Supplementary Figure 6). Previous investigations on the *in vitro* cytotoxic effect of aerosols generated from MCT, VEA, CBD/counterfeit vape cartridge, as well as nicotine and-based e-liquids, showed an overall dose- and time-dependent cell death and ROS generation, which were also correlated with e-liquid composition and aerosol generation parameters (puffing protocol, operational voltage) (Husari *et al.*, 2016; Jiang *et al.*, 2020; Lerner *et al.*, 2015; Matsumoto *et al.*, 2020; Muthumalage *et al.*, 2020b; Muthumalage and Rahman, 2019; Rowell *et al.*, 2017; Zhang *et al.*, 2021).

Exposure of epithelial cells to aerosols generated from Δ⁸THC/VEA e-liquids leads to mitochondrial dysfunction, expressed as a dose-dependent alteration of mitochondrial membrane potential, which did not correspond necessarily to activation of caspase-3 and apoptosis. Among the Δ⁸THC/VEA-based e-liquids, Δ⁸THC 36% + VEA 54% + Terp 10% at 3.7 and 5 V (loss ΔΨ_m > 20%), and Δ⁸THC 63% + VEA 27% + Terp 10% at 5 V (loss ΔΨ_m > 20%) induced the higher mitochondrial effect (Figure 7), whereas the activation of caspase 3 was only observed when cells were exposed to high doses of Δ⁸THC 36% + VEA 54% + Terp 10% aerosol (3.7 and 5 V), and both doses of VEA 100% (3.7 and 5 V) (Figure 7). In comparison, all nicotine-based e-liquids, as well as cigarette smoke, induced a significant dose-dependent alteration of the mitochondrial membrane potential and activation of the apoptosis cascade. This is in agreement with the current literature (Clapp *et al.*, 2019; Correia-Álvarez *et al.*, 2020; Zahedi *et al.*, 2019).

Finally, to better understand the link between the exposure of epithelial cells to aerosols generated from Δ⁸THC/VEA-based e-liquids and their inflammatory status, we measured the cytokines and chemokines released in the supernatant of epithelial cells exposed to the higher dose for 24 h. The results clarify that among the Δ⁸THC/VEA group the most bioactive aerosol was

Δ^8 THC 36% + VEA 54% + Terp 10% (3.7 and 5V), with effects similar to the nicotine group. Although most cytokines and chemokines were suppressed by all aerosols in both groups, the above-mentioned Δ^8 THC/VEA generated aerosols induced hypersecretion of FGF-2, G-CSF, GM-CSF, IL-1 α , IL-1RA, IL-18, MDC, PDGF-AB/BB, and suppression of GRO- α , TNF β , and VEGF-A (Figure 8).

Previous studies investigating the toxic effect of CBD, diluents, such as PG, VG, MCT, or VEA, or flavorings, such as menthol, cinnamaldehyde, either as e-liquid or aerosolized, showed a varying degree of cytotoxicity, barrier dysfunction, and inflammation both *in vitro* and *in vivo* depending on e-liquid composition, puffing protocol, operational voltage, and cell lines (Clapp et al., 2019; Crotty Alexander et al., 2018; Jiang et al., 2020; Leslie et al., 2017; Muthumalage et al., 2019; 2020b; Muthumalage and Rahman, 2019; Park et al., 2022; Phipps et al., 2010; Sundar et al., 2016). Although the most frequent biomarkers of e-cigs aerosol toxicity identified in biological samples are IL-1 β , IL-6, IL-8, IL-13 IFN- γ , MCP-1, MCSF, and TNF- α (Ghosh et al., 2019; Park et al., 2022; Scott et al., 2018; Shields et al., 2017; Sundar et al., 2016), clinical studies on acute lung injury have highlighted the critical role in the disease's development played by pro- and anti-inflammatory cytokines, such as IL-1 β , TNF- α , IL-1RA, and MIF, IL-8, found in the human BAL (Goodman et al., 2003). Laboratory findings in EVALI patients also showed elevated inflammatory markers (such as erythrocyte sedimentation rate, c-reactive protein, etc.), but the BAL outcomes found were mostly nonspecific, suggestive of a nonspecific inflammatory process (Blagev et al., 2019; Butt et al., 2019; Layden et al., 2020; Matsumoto et al., 2020; Muthumalage et al., 2020b; Triantafyllou et al., 2019). In the present study, aerosols generated from Δ^8 THC 36% + VEA 54% + Terp 10% (3.7 and 5V), but not from Δ^8 THC/terp or pure VEA, are as potent as aerosols generated from nicotine-based e-liquids in increasing a limited number of proinflammatory cytokines and suppressing the majority of them, whereas inducing a higher level of cytotoxicity.

This is one of the first studies to assess the *in vitro* acute toxic and inflammatory effect of aerosols generated from the combination of Δ^8 THC/VEA e-liquids on human lung epithelial cells and human monocytes aiming to find a causative agent for the development of EVALI. Previous studies focused on the *in vitro/in vivo* toxicological characterization of either parent e-liquids or aerosols generated from conventional nicotine, CBD alone, or nicotine/THC diluents, such as PG, VG, MCT, or VEA (Bhat et al., 2020; Jiang et al., 2020; Matsumoto et al., 2020; Muthumalage et al., 2020b; Muthumalage and Rahman, 2019) rather than the real-world combinations of the above. Their findings revealed that there is a considerable biological difference between the parent e-liquid and their aerosols and between aerosols generated from individual components and a mixture of e-liquids (Bhat et al., 2020; Jiang et al., 2020; Matsumoto et al., 2020; Muthumalage et al., 2020b; Muthumalage and Rahman, 2019). In agreement with the aforementioned literature, the present study confirms the different toxicological profiles correlated with the e-liquid composition (ie, VEA 100% vs Δ^8 THC 36% + VEA 54% + Terp 10%), but also with the operational voltage (ie, 3.7 and 5V). As evident from the real-time aerosol number-size distribution and time-integrated PM mass-size distribution, nearly all of the particles generated by vaping are in the fine particle size (<2.5 μ m), which means they are deposited in the deeper bronchioalveolar regions of the respiratory tract, where they could affect a range of adverse pulmonary outcomes depending on their chemical composition

(Lechasseur et al., 2019; Phipps et al., 2010; Xing et al., 2016; Zhai et al., 2022).

However, the *in vitro* cell models and exposure system applied in the present study have many intrinsic limitations: the single-cell monolayer does not account for the cell-to-cell interaction, presence of other stimuli, or underlying conditions, which are commonly present in the context of EVALI (Layden et al., 2020; Taylor et al., 2019); cells exposures in this study were large bolus doses of conditioned media generated with 85 and 257 puffs/m² of e-cig aerosol for 24 h, this submerged culture model does not completely recapitulate *in vivo* aerosol exposures, this dose is larger than a typical e-cig user would vape in that same period, and does not take into consideration clearance/repair mechanisms. Air-liquid interface (ALI) exposure systems can also be used to directly expose human airway epithelial cells to aerosols. In such a system, intact aerosol, including gaseous, semivolatile, and particle phases, is directly and intermittently delivered to the apical surface of the lung epithelial cells, mimicking the physiological airways exposure (Lacroix et al., 2018; Li, 2016; Upadhyay and Palmberg, 2018; Zavala et al., 2020). Although the findings of this study are not physiologically relevant compared with ALI or *in vivo* models, the use of *in vitro* cellular models, especially in comparative studies, provides useful information on endpoints of interest for understanding the associations between e-liquid composition/operational parameters and potential toxicity mechanisms in the development of EVALI.

In addition, a critical issue recognized in the aerosol collection is the potential loss of the major volatile toxicant contained in the gaseous phase of e-cig aerosols during bubbling, and the physicochemical alteration of toxicants due to reaction with media during the sampling process and in the timeframe between sampling and cell exposure. Moreover, Calu-3 human epithelial cells, used in place of primary human airways epithelial cells, are derived from a nonsmall-cell lung cancer cell line, were chosen for the initial and preliminary toxicological characterization of Δ^8 THC/VEA-derived aerosols, due to the rapid polarization in a stable culture that resembles the human lung epithelium-derived cells. They have also been extensively used in the toxicological assessment of e-cigs aerosol (Leslie et al., 2017; Rowell et al., 2017; Zhang et al., 2021).

Although this preliminary study focuses on the analysis of aerosols generated from "real-world" concentrations of Δ^8 THC/VEA/terpenes, including more controls, like Δ^8 THC alone, terpene alone, menthol alone, and PG/VG alone will be beneficial in the future for a more detailed physical, chemical, and toxicological characterization.

Other limitations in our study include the lack of deeper investigation on the role of macrophages in the development, progression, and resolution of the aggressive inflammatory process in EVALI. The involvement of both alveolar and interstitial macrophages in the EVALI syndrome is particularly important because they play a key role in the recognition and elimination of pathogens in the early stage (Higgins et al., 2008), and in the resolution of inflammation, regulation of fibroproliferative response, and wound healing in the late stage of disease (Bellingan, 2002; Gordon, 2003; Huang et al., 2018). Moreover, lipid-laden macrophages in the alveolar space were a common feature of the affected individuals (Christiani, 2020; Jonas, 2020).

These limitations are due to the fact that the present study focuses more on the human lung epithelial cells, as they represent a physical barrier that is disrupted by e-cigs aerosols in the EVALI syndrome. In this regard, it is crucial to evaluate the integrity of epithelial cell junctions, hence the epithelial barrier

dysfunction and permeability alteration, which in turn aggravates the inflammatory response, and facilitates the recruitment of the immune cells (Crotty Alexander et al., 2018; Muthumalage et al., 2019). Because our data show suppression of most cytokines following both Δ^8 THC and nicotine e-cig aerosols exposure, further studies using a more relevant cellular model are warranted to understand the mechanism of the immune modulation.

Furthermore, RNA-sequencing transcriptome analysis of the Calu-3 epithelial cells exposed to the e-cig aerosols is underway and we will report any mechanistic findings in a future manuscript.

CONCLUSION

This is one of the first studies to provide a comprehensive and systematic physicochemical and toxicological characterization of aerosols emitted from Δ^8 THC and VEA-based e-liquids, as they have been associated with the development of EVALI in the young healthy population in the United States in 2019–2020. The E-cig-EGS platform was used to generate real-world e-cig exposures for real-time monitoring and physicochemical and toxicological characterization of aerosols generated from combinations of different concentrations of Δ^8 THC + Terp with or without VEA and VEA 100% at 2 operational voltages (3.7 and 5V). Conventional nicotine-based e-liquids were also used as comparators. The main finding of the study is that e-liquid composition and operational voltage influenced the physicochemical properties of each aerosol (tPNC and size distribution, particulate mass-size distribution, release of VOC, and gaseous pollutants), as well as their biological and inflammatory effects (cell death, mitochondrial dysfunction, apoptosis, cytokines). Overall, the comparison between Δ^8 THC and nicotine e-liquid groups did not show particular differences, such that it was not possible to find a strong correlation between exposure to a specific aerosol generated from the Δ^8 THC/VEA group and the development of EVALI. Further organic chemical speciation of the aerosols is needed to identify chemical differences between aerosols generated between Δ^8 THC/VEA and nicotine-based e-liquid groups. However, the present study supports the concept that there was a significant difference between the individual e-liquid component (ie, VEA 100%) and the e-liquid mixture (ie, Δ^8 THC + VEA + Terp), in terms of both physicochemical characteristics and bioactivity. Therefore, it is fundamental, in the future, to avoid focusing on the toxicity of parent e-liquids or aerosols generated from individual diluents, as they do not reflect the real physicochemical exposure. The combination of chemicals can generate a mixture of toxicants whose synergistic actions can drive bioactivity and EVALI. Further comprehensive *in vitro/in vivo* inhalation studies, based also on a proteomic, genomic, and metabolomic approach, are necessary to validate the *in vitro* toxicological effects and to address the specific cascade of events that leads to diffuse alveolar damage and respiratory failure in EVALI patients. Findings from this study will help risk assessors, and public health and governmental agencies, for the development of Δ^8 THC and nicotine e-cig regulations, to limit the epidemic of e-cigs in the young population and prevent new cases of EVALI due to the incorporation of unregulated chemicals in e-cigs.

SUPPLEMENTARY DATA

Supplementary data are available at Toxicological Sciences online.

FUNDING

This investigation was made possible by the T32 grant no. HL007118 from NIH. The cytokine/chemokines analysis was made possible by grant no. P30ES000002 from the Integrated Health Sciences Facility (IHSFC) of the Harvard NIEHS Center for Environmental Health. The e-cigs cartridges and Δ^8 THC e-liquids were kindly provided by Jeff Rawson PhD, Postdoctoral Fellow from Prof. George M. Whitesides Laboratory, Department of Chemistry and Chemical Biology, Harvard University.

DECLARATION OF CONFLICTING INTERESTS

The authors declared no potential conflicts of interest with respect to the research, authorship, and/or publication of this article.

REFERENCES

- Bellingan, G. J. (2002). The pulmonary physician in critical care 6: The pathogenesis of ALI/ARDS. *Thorax* 57, 540–546.
- Bhat, T. A., Kalathil, S. G., Bogner, P. N., Blount, B. C., Goniewicz, M. L., and Thanavala, Y. M. (2020). An animal model of inhaled vitamin E acetate and EVALI-like lung injury. *N. Engl. J. Med.* 382, 1175–1177.
- Blagev, D. P., Harris, D., Dunn, A. C., Guidry, D. W., Grissom, C. K., and Lanspa, M. J. (2019). Clinical presentation, treatment, and short-term outcomes of lung injury associated with e-cigarettes or vaping: A prospective observational cohort study. *Lancet* 394, 2073–2083.
- Blount, B. C., Karwowski, M. P., Morel-Espinosa, M., Rees, J., Sosnoff, C., Cowan, E., Gardner, M., Wang, L., Valentin-Blasini, L., Silva, L., et al. (2019). Evaluation of bronchoalveolar lavage fluid from patients in an outbreak of e-cigarette, or vaping, product use-associated lung injury - 10 states, August–October 2019. *MMWR Morb. Mortal. Wkly. Rep.* 68, 1040–1041.
- Blount, B. C., Karwowski, M. P., Shields, P. G., Morel-Espinosa, M., Valentin-Blasini, L., Gardner, M., Braselton, M., Brosius, C. R., Caron, K. T., Chambers, D., Lung Injury Response Laboratory Working Group, et al. (2020). Vitamin E acetate in bronchoalveolar-lavage fluid associated with EVALI. *N. Engl. J. Med.* 382, 697–705.
- Butt, Y. M., Smith, M. L., Tazelaar, H. D., Vaszar, L. T., Swanson, K. L., Cecchini, M. J., Boland, J. M., Bois, M. C., Boyum, J. H., Froemming, A. T., et al. (2019). Pathology of vaping-associated lung injury. *N. Engl. J. Med.* 381, 1780–1781.
- Centers for Disease Control and Prevention (CDC). (2019). For state, local, territorial, and tribal health departments. Electronic cigarettes. Smoking & tobacco use. 2019 lung injury surveillance primary case definition (CDC), September 18, 2019. Available at: https://www.cdc.gov/tobacco/basic_information/e-cigarettes/severe-lung-disease/health-departments/index.html.
- Centers for Disease Control and Prevention (CDC). (2020). Outbreak of lung injury associated with the use of e-cigarette, or vaping, products. Available at: https://www.cdc.gov/tobacco/basic_information/e-cigarettes/severe-lung-disease.html. Accessed November 27, 2020.
- CDC U.S. Department of Health and Human Services. (2016). E-cigarette use among youth and young adults: A report of the surgeon general. Atlanta, GA.

- Christiani, D. C. (2020). Vaping-induced lung injury. *N. Eng. J. Med.* **382**, 960–962.
- Clapp, P. W., Lavrich, K. S., van Heusden, C. A., Lazarowski, E. R., Carson, J. L., and Jaspers, I. (2019). Cinnamaldehyde in flavored e-cigarette liquids temporarily suppresses bronchial epithelial cell ciliary motility by dysregulation of mitochondrial function. *Am. J. Physiol. Lung Cell. Mol. Physiol.* **237**, L470–L486.
- Correia-Álvarez, E., Keating, J. E., Glish, G., Tarran, R., and Sassano, M. F. (2020). Reactive oxygen species, mitochondrial membrane potential, and cellular membrane potential are predictors of e-liquid induced cellular toxicity. *Nicotine Tob. Res.* **22**, S4–S13.
- Crotty Alexander, L. E., Drummond, C. A., Hepokoski, M., Mathew, D., Moshensky, A., Willeford, A., Das, S., Singh, P., Yong, Z., Lee, J. H., et al. (2018). Chronic inhalation of e-cigarette vapor containing nicotine disrupts airway barrier function and induces systemic inflammation and multiorgan fibrosis in mice. *Am. J. Physiol. Regul. Integr. Comp. Physiol.* **314**, R834–R847.
- Demokritou, P., Lee, S. J., Ferguson, S. T., and Koutrakis, P. (2004). A compact multistage (cascade) impactor for the characterization of atmospheric aerosols. *J. Aerosol Sci.* **35**, 281–299.
- Duffy, B., Li, L., Lu, S., Durocher, L., Dittmar, M., Delaney-Baldwin, E., Panawennage, D., LeMaster, D., Navarette, K., and Spink, D. (2020). Analysis of cannabinoid-containing fluids in illicit vaping cartridges recovered from pulmonary injury patients: Identification of vitamin E acetate as a major diluent. *Toxics* **8**, 8.
- Etter, J. F., and Bullen, C. (2011). Electronic cigarette: Users profile, utilization, satisfaction and perceived efficacy. *Addiction* **106**, 2017–2028.
- Farsalinos, K. E., Romagna, G., Alliffranchini, E., Ripamonti, E., Bocchietto, E., Todeschi, S., Tsiapras, D., Kyrzopoulos, S., and Voudris, V. (2013a). Comparison of the cytotoxic potential of cigarette smoke and electronic cigarette vapour extract on cultured myocardial cells. *Int. J. Environ. Res. Public Health* **10**, 5146–5162.
- Farsalinos, K. E., Romagna, G., Tsiapras, D., Kyrzopoulos, S., and Voudris, V. (2013b). Evaluation of electronic cigarette use (vaping) topography and estimation of liquid consumption: Implications for research protocol standards definition and for public health authorities' regulation. *Int. J. Environ. Res. Public Health* **10**, 2500–2514.
- FDA. (2020). Lung illnesses associated with use of vaping products. Available at: <https://www.fda.gov/news-events/public-health-focus/lung-injuries-associated-use-vaping-products>.
- Fuoco, F. C., Buonanno, G., Stabile, L., and Vigo, P. (2014). Influential parameters on particle concentration and size distribution in the mainstream of e-cigarettes. *Environ. Pollut.* **184**, 523–529.
- Geiss, O., Bianchi, I., and Barrero-Moreno, J. (2016). Correlation of volatile carbonyl yields emitted by e-cigarettes with the temperature of the heating coil and the perceived sensorial quality of the generated vapours. *Int. J. Hyg. Environ. Health* **219**, 268–277.
- Ghosh, A., Coakley, R. D., Ghio, A. J., Muhlebach, M. S., Esther, C. R., Jr, Alexis, N. E., and Tarran, R. (2019). Chronic e-cigarette use increases neutrophil elastase and matrix metalloproteinase levels in the lung. *Am. J. Resp. Crit. Care Med.* **200**, 1392–1401.
- Goodman, R. B., Pugin, J., Lee, J. S., and Matthay, M. A. (2003). Cytokine-mediated inflammation in acute lung injury. *Cytokine Growth Factor Rev.* **14**, 523–535.
- Gordon, S. (2003). Alternative activation of macrophages. *Nat. Rev. Immunol.* **3**, 23–35.
- Higgins, D. M., Sanchez-Campillo, J., Rosas-Taraco, A. G., Higgins, J. R., Lee, E. J., Orme, I. M., and Gonzalez-Juarrero, M. (2008). Relative levels of M-CSF and GM-CSF influence the specific generation of macrophage populations during infection with mycobacterium tuberculosis. *J. Immunol.* **180**, 4892–4900.
- Huang, X., Xiu, H., Zhang, S., and Zhang, G. (2018). The role of macrophages in the pathogenesis of ALI/ARDS. *Mediators Inflamm.* **2018**, 1264913.
- Husari, A., Shihadeh, A., Talih, S., Hashem, Y., El Sabban, M., and Zaatari, G. (2016). Acute exposure to electronic and combustible cigarette aerosols: Effects in an animal model and in human alveolar cells. *Nicotine Tob Res.* **18**, 613–619.
- Ingebretsen, B. J., Cole, S. K., and Alderman, S. L. (2012). Electronic cigarette aerosol particle size distribution measurements. *Inhal. Toxicol.* **24**, 976–984.
- Invernizzi, G., Ruprecht, A., De Marco, C., Paredi, P., and Boffi, R. (2007). Residual tobacco smoke: Measurement of its washout time in the lung and of its contribution to environmental tobacco smoke. *Tob. Control.* **16**, 29–33.
- Jiang, H., Ahmed, C. M. S., Martin, T. J., Canchola, A., Oswald, I. W. H., Garcia, J. A., Chen, J. Y., Koby, K. A., Buchanan, A. J., Zhao, Z., et al. (2020). Chemical and toxicological characterization of vaping emission products from commonly used vape juice diluents. *Chem. Res. Toxicol.* **33**, 2157–2163.
- Jonas, A. (2020). Lipid-laden alveolar macrophages and vaping: Lessons from EVALI. *EBioMedicine* **60**, 103010.
- Ko, T. J., and Kim, S. A. (2022). Effect of heating on physicochemical property of aerosols during vaping. *Int. J. Environ. Res. Public Health* **19**, 1892.
- Kosmider, L., Jackson, A., Leigh, N., O'Connor, R., and Goniewicz, M. L. (2018). Circadian puffing behavior and topography among e-cigarette users. *Tob. Regul. Sci.* **4**, 41–49.
- Lacroix, G., Koch, W., Ritter, D., Gutleb, A. C., Larsen, S. T., Loret, T., Zanetti, F., Constant, S., Chortarea, S., Rothen-Rutishauser, B., et al. (2018). Air-liquid interface in vitro models for respiratory toxicology research: Consensus workshop and recommendations. *Appl. In Vitro Toxicol.* **4**, 91–106.
- Lamos, S., Kostenidou, E., Farsalinos, K., Zagoriti, Z., Ntoukas, A., Dalamarinis, K., Savranakis, P., Lagoumintzis, G., and Poulas, K. (2019). Real-time assessment of e-cigarettes and conventional cigarettes emissions: Aerosol size distributions, mass and number concentrations. *Toxics* **7**, 45.
- Lanzarotta, A., Falconer, T. M., Flurer, R., and Wilson, R. A. (2020). Hydrogen bonding between tetrahydrocannabinol and vitamin E acetate in unvaped, aerosolized, and condensed aerosol e-liquids. *Anal. Chem.* **92**, 2374–2378.
- Layden, J. E., Ghinai, I., Pray, I., Kimball, A., Layer, M., Tenforde, M. W., Navon, L., Hoots, B., Salvatore, P. P., Elderbrook, M., et al. (2020). Pulmonary illness related to e-cigarette use in Illinois and Wisconsin - final report. *N. Engl. J. Med.* **382**, 903–916.
- Lechasseur, A., Altmejd, S., Turgeon, N., Buonanno, G., Morawska, L., Brunet, D., Duchaine, C., and Morissette, M. C. (2019). Variations in coil temperature/power and e-liquid constituents change size and lung deposition of particles emitted by an electronic cigarette. *Physiol. Rep.* **7**, e14093.
- Lerner, C. A., Sundar, I. K., Yao, H., Gerloff, J., Ossip, D. J., McIntosh, S., Robinson, R., and Rahman, I. (2015). Vapors produced by electronic cigarettes and e-juices with flavorings induce toxicity, oxidative stress, and inflammatory response

- in lung epithelial cells and in mouse lung. *PLoS One* **10**, e0116732.
- Leslie, L. J., Vasanthi Bathrinarayanan, P., Jackson, P., Mabiala Ma Muanda, J. A., Pallett, R., Stillman, C. J., and Marshall, L. J. (2017). A comparative study of electronic cigarette vapor extracts on airway-related cell lines in vitro. *Inhal. Toxicol.* **29**, 126–136.
- Li, X. (2016). In vitro toxicity testing of cigarette smoke based on the air-liquid interface exposure: A review. *Toxicol. In Vitro* **36**, 105–113.
- Matsumoto, S., Fang, X., Traber, M. G., Jones, K. D., Langelier, C., Hayakawa Serpa, P., Calfee, C. S., Matthay, M. A., and Gotts, J. E. (2020). Dose-dependent pulmonary toxicity of aerosolized vitamin E acetate. *Am. J. Respir. Cell Mol. Biol.* **63**, 748–757.
- Meehan-Atrash, J., Luo, W., McWhirter, K. J., and Strongin, R. M. (2019). Aerosol gas-phase components from cannabis e-cigarettes and dabbing: Mechanistic insight and quantitative risk analysis. *ACS Omega* **4**, 16111–16120.
- Mikheev, V. B., Brinkman, M. C., Granville, C. A., Gordon, S. M., and Clark, P. I. (2016). Real-time measurement of electronic cigarette aerosol size distribution and metals content analysis. *Nicotine Tob. Res.* **18**, 1895–1902.
- Mikheev, V. B., Klupinski, T. P., Ivanov, A., Lucas, E. A., Strozier, E. D., and Fix, C. (2020). Particle size distribution and chemical composition of the aerosolized vitamin E acetate. *Aerosol. Sci. Technol.* **54**, 993–998.
- Muthumalage, T., Friedman, M. R., McGraw, M. D., Ginsberg, G., Friedman, A. E., and Rahman, I. (2020a). Chemical constituents involved in e-cigarette, or vaping product use-associated lung injury (EVALI). *Toxics* **8**, 25.
- Muthumalage, T., Lamb, T., Friedman, M. R., and Rahman, I. (2019). E-cigarette flavored pods induce inflammation, epithelial barrier dysfunction, and DNA damage in lung epithelial cells and monocytes. *Sci. Rep.* **9**, 19035.
- Muthumalage, T., Lucas, J. H., Wang, Q., Lamb, T., McGraw, M. D., and Rahman, I. (2020b). Pulmonary toxicity and inflammatory response of e-cigarette vape cartridges containing medium-chain triglycerides oil and vitamin E acetate: Implications in the pathogenesis of EVALI. *Toxics* **8**, 46.
- Muthumalage, T., and Rahman, I. (2019). Cannabidiol differentially regulates basal and lps-induced inflammatory responses in macrophages, lung epithelial cells, and fibroblasts. *Toxicol. Appl. Pharmacol.* **382**, 114713.
- NIDA. (2021, September 20). CDC health advisory: Increases in availability of cannabis products containing delta-8 THC and reported cases of adverse events. Available at: <https://nida.nih.gov/news-events/emerging-trend/cdc-health-advisory-increases-in-availability-cannabis-products-containing-delta-8-thc-reported>. Accessed March 4, 2022.
- Pal, A. K., Watson, C. Y., Pirela, S. V., Singh, D., Chalbot, M. C., Kavouras, I., and Demokritou, P. (2015). Linking exposures of particles released from nano-enabled products to toxicology: An integrated methodology for particle sampling, extraction, dispersion, and dosing. *Toxicol. Sci.* **146**, 321–333.
- Park, J. A., Crotty Alexander, L. E., and Christiani, D. C. (2022). Vaping and lung inflammation and injury. *Annu. Rev. Physiol.* **84**, 611–629.
- Phipps, J. C., Aronoff, D. M., Curtis, J. L., Goel, D., O'Brien, E., and Mancuso, P. (2010). Cigarette smoke exposure impairs pulmonary bacterial clearance and alveolar macrophage complement-mediated phagocytosis of *Streptococcus pneumoniae*. *Inf. Immun.* **78**, 1214–1220.
- Rowell, T. R., Reeber, S. L., Lee, S. L., Harris, R. A., Nethery, R. C., Herring, A. H., Glish, G. L., and Tarran, R. (2017). Flavored e-cigarette liquids reduce proliferation and viability in the Calu3 airway epithelial cell line. *Am. J. Physiol. Lung Cell. Mol. Physiol.* **313**, L52–L66.
- Scott, A., Lugg, S. T., Aldridge, K., Lewis, K. E., Bowden, A., Mahida, R. Y., Grudzinska, F. S., Dosanjh, D., Parekh, D., Foronjy, R., et al. (2018). Pro-inflammatory effects of e-cigarette vapour condensate on human alveolar macrophages. *Thorax* **73**, 1161–1169.
- Scungio, M., Stabile, L., and Buonanno, G. (2018). Measurements of electronic cigarette-generated particles for the evaluation of lung cancer risk of active and passive users. *J. Aerosol. Sci.* **115**, 1–11.
- Shields, P. G., Berman, M., Brasky, T. M., Freudenheim, J. L., Mathe, E., McElroy, J. P., Song, M.-A., and Wewers, M. D. (2017). A review of pulmonary toxicity of electronic cigarettes in the context of smoking: A focus on inflammation. *Cancer Epidemiol. Prevent. Biomark* **26**, 1175–1191.
- Singh, D., Marrocco, A., Wohlleben, W., Park, H.-R., Diwadkar, A. R., Himes, B. E., Lu, Q., Christiani, D. C., and Demokritou, P. (2022). Release of particulate matter from nano-enabled building materials (NEBMS) across their lifecycle: Potential occupational health and safety implications. *J. Haz. Mat.* **422**, 126771.
- Sundar, I. K., Javed, F., Romanos, G. E., and Rahman, I. (2016). E-cigarettes and flavorings induce inflammatory and pro-senescence responses in oral epithelial cells and periodontal fibroblasts. *Oncotarget* **7**, 77196–77204.
- Tackett, A. P., Lechner, W. V., Meier, E., Grant, D. M., Driskill, L. M., Tahirkheli, N. N., and Wagener, T. L. (2015). Biochemically verified smoking cessation and vaping beliefs among vape store customers. *Addiction* **110**, 868–874.
- Taylor, J., Wiens, T., Peterson, J., Saravia, S., Lunda, M., Hanson, K., Wogen, M., D'Heilly, P., Margetta, J., Bye, M., et al.; Lung Injury Response Task Force. (2019). Characteristics of e-cigarette, or vaping, products used by patients with associated lung injury and products seized by law enforcement - Minnesota, 2018 and 2019. *MMWR Morb. Mortal. Wkly. Rep.* **68**, 1096–1100.
- Triantafyllou, G. A., Tiberio, P. J., Zou, R. H., Lamberty, P. E., Lynch, M. J., Kreit, J. W., Gladwin, M. T., Morris, A., and Chiarichiaro, J. (2019). Vaping-associated acute lung injury: A case series. *Am. J. Respir. Crit. Care Med.* **200**, 1430–1431.
- Upadhyay, S., and Palmberg, L. (2018). Air-liquid interface: Relevant in vitro models for investigating air pollutant-induced pulmonary toxicity. *Toxicol. Sci.* **164**, 21–30.
- Xing, Y. F., Xu, Y. H., Shi, M. H., and Lian, Y. X. (2016). The impact of PM2.5 on the human respiratory system. *J. Thorac. Dis.* **8**, E69–E74.
- Zahedi, A., Phandthong, R., Chaili, A., Leung, S., Omaiye, E., and Talbot, P. (2019). Mitochondrial stress response in neural stem cells exposed to electronic cigarettes. *iScience* **16**, 250–269.
- Zavala, J., Freedman, A. N., Szilagyi, J. T., Jaspers, I., Wambaugh, J. F., Higuchi, M., and Rager, J. E. (2020). New approach methods to evaluate health risks of air pollutants: Critical design considerations for in vitro exposure testing. *Int. J. Environ. Res. Public Health* **17**, 2124.
- Zhai, X., Wang, J., Sun, J., and Xin, L. (2022). PM(2.5) induces inflammatory responses via oxidative stress-mediated mitophagy in human bronchial epithelial cells. *Toxicol. Res.* **11**, 195–205.
- Zhang, R., Jones, M. M., Dornsife, R. E., Wu, T., Sivaraman, V., Tarran, R., and Onyenwoke, R. U. (2021). JUUL e-liquid exposure elicits cytoplasmic Ca²⁺ responses and leads to cytotoxicity in cultured airway epithelial cells. *Toxicol. Lett.* **337**, 46–56.

- Zhang, Y., Sumner, W., and Chen, D. R. (2013). In vitro particle size distributions in electronic and conventional cigarette aerosols suggest comparable deposition patterns. *Nicotine Tob. Res.* **15**, 501–508.
- Zhao, J., Nelson, J., Dada, O., Pyrgiotakis, G., Kavouras, I. G., and Demokritou, P. (2018a). Assessing electronic cigarette emissions: Linking physico-chemical properties to product brand, e-liquid flavoring additives, operational voltage and user puffing patterns. *Inhal. Toxicol.* **30**, 78–88.
- Zhao, J., Pyrgiotakis, G., and Demokritou, P. (2016). Development and characterization of electronic-cigarette exposure generation system (Ecig-EGS) for the physico-chemical and toxicological assessment of electronic cigarette emissions. *Inhal. Toxicol.* **28**, 658–669.
- Zhao, J., Zhang, Y., Sisler, J. D., Shaffer, J., Leonard, S. S., Morris, A. M., Qian, Y., Bello, D., and Demokritou, P. (2018b). Assessment of reactive oxygen species generated by electronic cigarettes using acellular and cellular approaches. *J. Hazard. Mater.* **344**, 549–557.